AN ABSTRACT OF THE THESIS OF

Samuel Seiji Matsuo for the Doctor of Philosophy
(Name) (Degree)

in Electrical Engineering presented on July 5, 1967
(Major) (Date)

Title: Properties of Flash-Evaporated Gallium Arsenide and Gallium Phosphide Epitaxial Films

Abstract approved: [redacted]
James C. Looney

The properties of flash-evaporated films of GaAs and GaP were studied in this investigation. Films were grown at various substrate temperatures, source temperatures, source-to-substrate distances and rates of deposition and were evaluated as to their structural, optical and electric properties.

It was found that substrate temperature was the major factor in determining the crystallinity of the films. Films deposited below about 250°C were found to be amorphous. As the substrate temperature was increased, the crystallinity of the films improved.

The optical data showed that the films had band gaps in the range of 1.34 to 1.72 ev. for GaAs films. Temperature-versus-resistivity measurements showed that the band gap for GaAs films varied from 1.18 ev. to 1.72 ev. The value for bulk GaAs is 1.47 ev.

Films grown from evaporant powders obtained by crushing wafers of 6×10^{-3} ohm-cm to 0.01 ohm-cm material had very high resistivities. To lower film resistivity, additional doping was incorporated in the evaporant. Tin was added to n-type wafers and zinc to p-type wafers. The films grown from the tin-rich evaporant powders showed a decrease in resistivity for an increase in tin concentration and an increase in resistivity for a decrease in substrate temperature. Films grown from zinc-rich powders had high resistivities in all cases.

Hall measurements were made but most films showed no voltage above the noise level of the measuring apparatus. The highest mobility value calculated from those films that exhibited Hall voltage was 0.7 cm^2/volt-sec, far below the value of 8500 cm^2/volt-sec for bulk GaAs.

Electroluminescence was noted in high-resistivity GaP films grown on GaAs substrates. A wide spectral emission energy band was measured which would indicate an avalanche process as being the carrier injection mechanism.

Point-contact and evaporated diodes were fabricated from the flash-evaporated films. Large leakage currents were noted in both types of diodes.

PROPERTIES OF FLASH-EVAPORATED GALLIUM ARSENIDE

AND

GALLIUM PHOSPHIDE EPITAXIAL FILMS

by

SAMUEL SEIJI MATSUO

A THESIS

submitted to

OREGON STATE UNIVERSITY

in partial fulfillment
of the requirements for the
degree of

DOCTOR OF PHILOSOPHY

June 1968

APPROVED:

[redacted]

Associate Professor of Department of Electrical and Electronics Engineering in charge of major

[redacted]

Head of Department of Electrical and Electronics Engineering

[redacted]

Dean of Graduate School

Date thesis is presented July 5, 1967

Typed by Erma McClanathan for Samuel Seiji Matsuo

ACKNOWLEDGMENTS

The author wishes to express his very sincere and deep appreciation to Professor James C. Looney for his continuous guidance and constructive criticism during the course of this research.

Gratitude is also expressed to Mr. Gene Hansen of Tektronix, Inc. for obtaining the x-ray data.

TABLE OF CONTENTS

	Page
Introduction	1
Plan of Presentation	2
Methods of Growing III-V Epitaxial Semiconductor Films	2
Theoretical Discussion	10
Crystal Structure	10
Crystal Growth	13
The Flash-Evaporation Method	23
Optical Properties of Semiconductors	26
Electrical Properties of Semiconductors	29
Electroluminescence	33
Experimental Apparatus and Procedure	37
The Pumping System	37
Source Heater	40
Substrate Heater	43
Particle-Feed System	44
Substrate Preparation	47
Source Material Preparation	48
The Evaporation Procedure	48
Experimental Results	51
Crystallinity of Evaporated Films	51
Optical Measurements	54
High-Resistivity Films	56
Low-Resistivity Films	60
Hall Effect	66
Diode Action	67
Light Emission in GaP Semi-Insulating Films	70

Discussion of Results and Summary..... 75

Optical Properties..... 75

High-Resistivity Films..... 77

Low-Resistivity Films..... 79

Hall Effect..... 80

Electroluminescence..... 81

Summary..... 82

Bibliography..... 88

LIST OF FIGURES

Figure		Page
1.	Experimental Apparatus Used by Kurov and Pinsker for Preparing InSb	4
2.	Experimental Apparatus Used by Davey and Pankey for Growing Epitaxial GaAs Films	6
3.	Zinc-Blende Crystal Structure of GaAs	11
4.	Lattice Constants for Various Compositions of GaAs-GaP Systems	13
5.	Relative Energy Variation Along a Linear Path on a Substrate Surface	19
6.	Positions of Different Bonding Energies in a Crystal Lattice	20
7.	Variations of the Condensation Coefficient with Substrate Temperature	21
8.	Absorption Coefficient of N-Type GaAs for Three Samples of Different Doping	27
9.	Temperature Dependence of Conductance for GaAs Samples of Different Doping	32
10.	Electroluminescent Spectral Response of a Reverse-Biased Alloyed GaP Diode at 300°K	35
11.	Arrangement of Vacuum System Components	38
12.	Internal Structure of the Varian Sputter-Ion Pump	39
13.	The Three Basic Types of Source Heaters Used	41
14.	Ceramic Disc Heater Used for Substrate Heating	43
15.	Tubular Oven Used as the Substrate Heater	45
16.	Experimental Setup Using the Ceramic Disc Substrate Heater and the Horizontal Source Heater	50

Figure Page

17. Fluorescence Curves Used to Determine Film Stoichiometry..... 53

18. Optical Absorption Coefficient Versus Energy of Incident Light for Low-Resistivity Films..... 55

19. V-I Characteristics of High-Resistivity GaAs Films Grown on a Germanium Substrate.. 57

20. Resistivity Versus Percent Tin for GaAs Films Grown at a Substrate Temperature of 570°C..... 61

21. Resistivity Versus Substrate Temperature for GaAs Films with 3.2% Tin in the Evaporant Material..... 62

22. Temperature Dependence of Low-Resistivity Flash-Evaporated GaAs Films Grown on Sapphire Substrates..... 64

23. Expanded Graph of the Intrinsic Portion of the Curves Shown in Figure 22..... 65

24. V-I Characteristics for a Point-Contact Diode on a Film Deposited from GaAs Powder Containing 4.5% Tin..... 68

25. V-I Characteristics of a Diode Grown by Evaporating 4.5% Tin-Doped GaAs on a P-Type Substrate..... 69

26. Block Diagram of the Apparatus Used to Measure the Light Emission Spectrum from High-Resistivity GaP Films..... 71

27. Spectral Response Curves for a Tungsten Filament at 1670°C and the Light Emitted by a High-Resistivity GaP Film..... 72

28. Typical V-I Curves for the Electro-luminescent Devices Studied..... 73

29. Zinc-Blende Lattice Showing a 60° Dislocation..... 78

LIST OF TABLES

Table Page

I. Growth Conditions and Breakdown Voltage for Some High-Resistivity Epitaxial GaAs Films 58

PROPERTIES OF FLASH-EVAPORATED GALLIUM ARSENIDE AND GALLIUM PHOSPHIDE EPITAXIAL FILMS

I. INTRODUCTION

This project is concerned with the growing of epitaxial GaAs and GaP films by flash evaporation on substrates of germanium, GaAs and sapphire and with the evaluation of the properties of these films. Interest in the epitaxial growth of thin film semiconductors is due to the additional latitude in design that is gained by employing this technique. For instance, devices fabricated on single wafers have inherent coupling problems. This can be alleviated by growing semiconductor films on insulating substrates and using these substrates as the isolation media.

Epitaxial films of silicon and germanium have received the major portion of past efforts. However, III-V compound semiconductors are also of interest because of their particular electrical properties such as higher electron mobilities, larger Hall effect voltages and wider range of band gaps.

In this investigation the effects of the source temperature, the substrate temperature, the source-to-substrate distance, the type of substrate and the rate of deposition on crystal growth were studied. The films

were evaluated as to their structural, optical and electrical properties. PN junctions were grown under various conditions and evaluated. Electroluminescence of the films was also investigated.

Plan of Presentation

The plan of presentation will be to consider crystal, optical and electrical theory of semiconductors in Chapter Two following the introductory Chapter One. Chapter Three will discuss the experimental apparatus and procedures used, and Chapter Four will present the results of the experiment. In the final chapter, a discussion of the results and a summary of the important findings will be presented.

Methods of Growing III-V Epitaxial Semiconductor Films

Purification, synthesis and growth of III-V semiconductor materials has been much more difficult than for the elemental semiconductors. The difficulty primarily arises from the different vapor pressures of the constituents of the compounds. In GaAs, for example, the arsenic pressure is 0.9 atmospheres at its melting point of 1235°C, while for GaP, phosphorus has a vapor pressure of 30 atmospheres at 1465°C, its melting point. The gallium vapor pressure is 10^{-4} atmospheres and

$3x10^{-3}$ atmospheres respectively at the melting points of these materials.

Several methods have been proposed in the past for growing III-V epitaxial films. One of the original methods was to evaporate the constituents of the compound separately. By controlling the temperatures of the two sources, the desired vapor flux could theoretically be obtained.

In one of the earlier experiments, Kurov and Pinsker (52) were able to prepare InSb in this manner. Their experimental apparatus is shown in Figure 1. The film dimensions have been purposely drawn out of scale to illustrate the method in which they were able to obtain proper stoichiometry. Due to the finite distance between the two sources, the vapor flux reaching the substrate was not entirely uniform. It was alternately richer in one component at the edges, but somewhere in between the proper conditions were met by the impinging molecules so that stoichiometric InSb was deposited. The substrate temperature during deposition was 20°C. The films were annealed for two hours at 100°C to 120°C and by use of electron diffraction pattern the composition of the film at various points was determined. Presnov and Synov (52) successfully evaporated films of AlSb, InSb and GaSb in this manner.

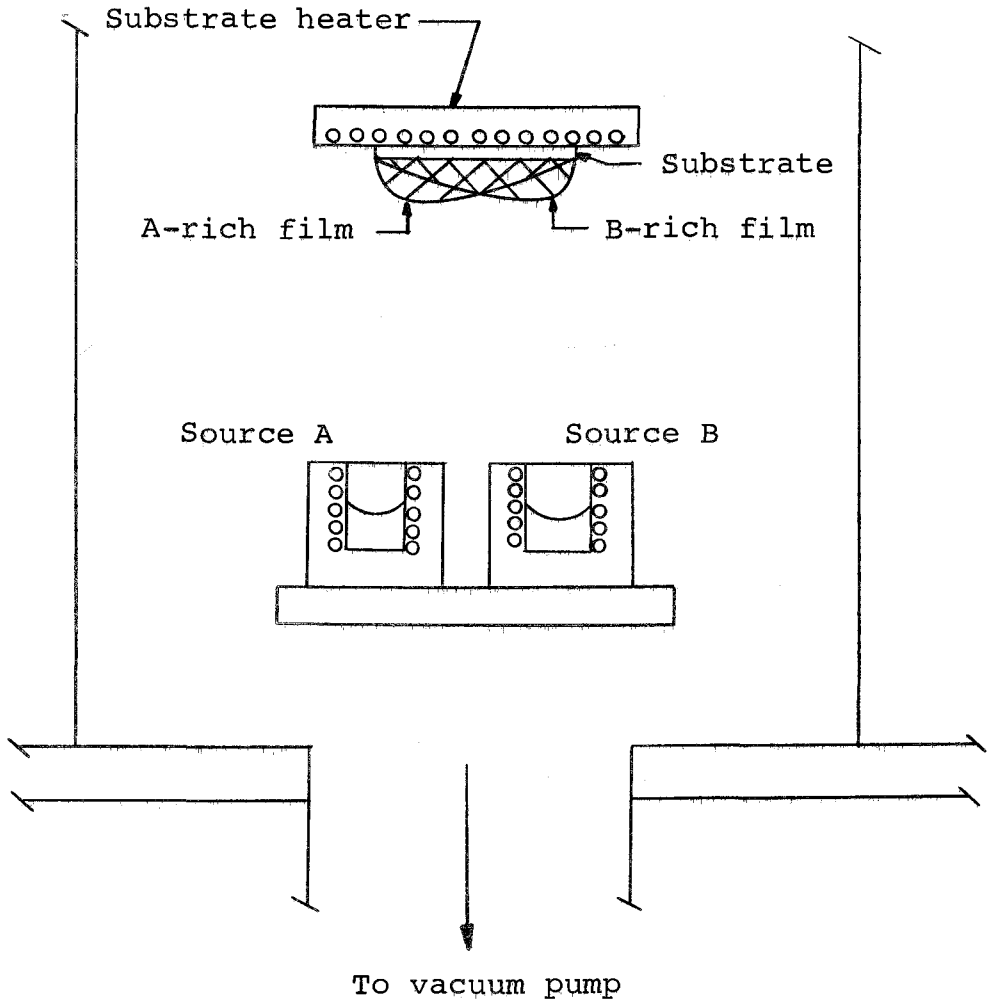

Figure 1. Experimental apparatus used by Kurov and Pinsker for preparing InSb (52).

More recently Davey and Pankey (11) used this three-temperature method to grow films of GaAs. Their apparatus differed in several respects as shown in Figure 2. The major difference is that direct source-to-substrate deposition is not used. Instead the atmosphere surrounding the substrate is controlled so that stoichiometric growth is obtained. The technique was originally proposed by Gunther (52).

The proper experimental conditions as determined by Davey and Pankey were to hold the gallium oven at 940°C, the arsenic oven at 295°C and the main oven at 150°C. They used a range of substrate temperatures varying from 175°C to 450°C and found that on quartz substrates films deposited below 220°C were amorphous while films deposited above this temperature were polycrystalline. They also found that between 250°C and 300°C, a low resistivity value of 30 ohm-cm was obtained. Above 300°C and below 250°C the films had resistivities of greater than 10^8 ohm-cm.

Another of the earlier methods proposed was to evaporate the compound itself and anneal the evaporated film. Paparoditis (52) reported films of InSb and InAs successfully evaporated in this manner. However, a critical film thickness of 600 Å was noted. For films thicker than this, the annealing step did not produce the

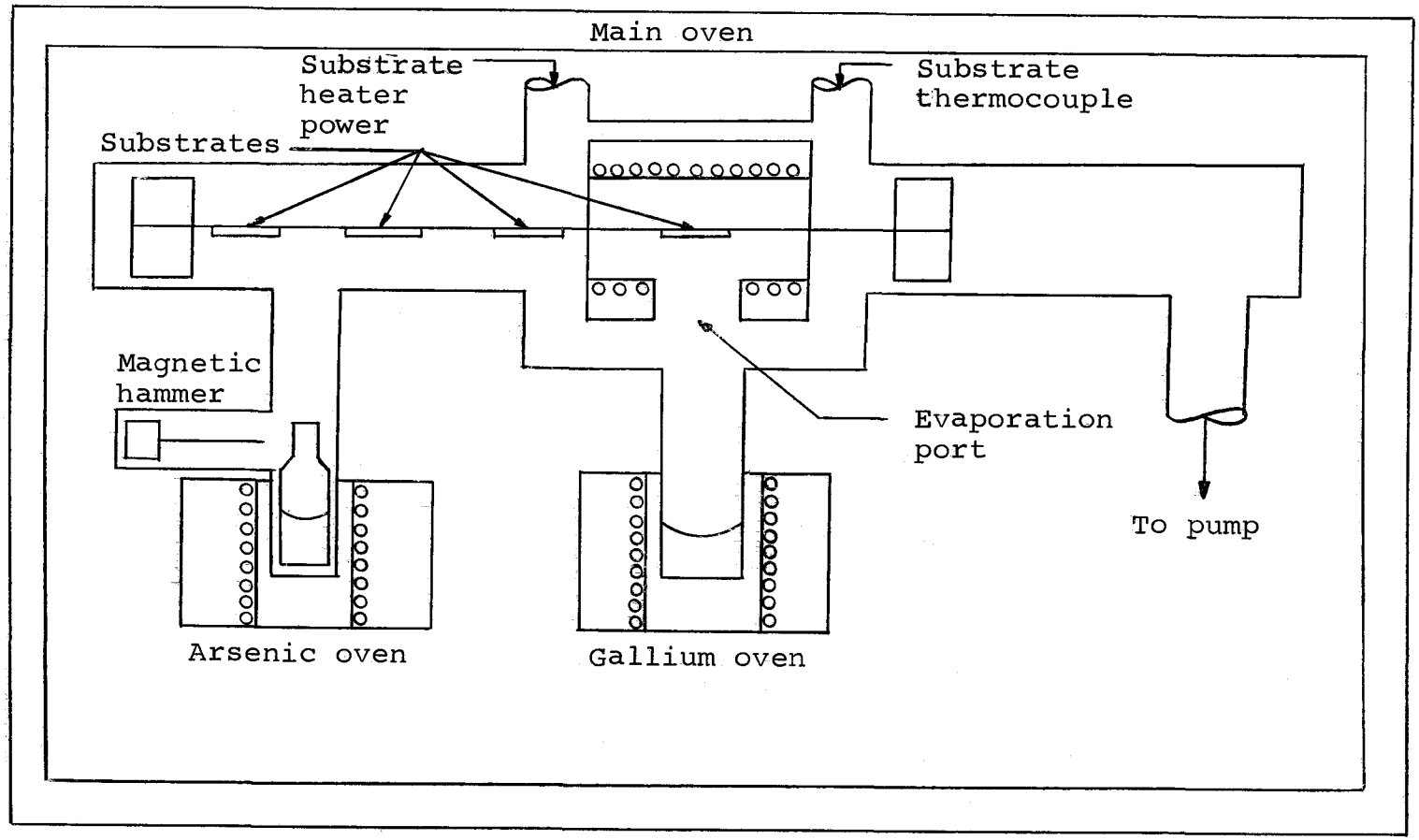

Figure 2. Experimental apparatus used by Davey and Pankey for growing epitaxial GaAs films.

proper rearrangement of atoms.

Recently, three other methods have come under consideration. These are the vapor-transport method, the sputtering method and the flash-, or instantaneous-, evaporation method.

The vapor-growth method can be further divided into the two categories, the closed-tube method and the open-tube method. In the closed-tube method a reaction of the type

$$3GaCl_{(g)} + \frac{1}{2} As_{4(g)} \rightleftharpoons GaCl_{3(g)} + 2GaAs_{(s)}$$

is used. The source is located at one end of the tube and the substrate of the other. The temperatures at the ends of the tube are such that the above reaction will go to the right on the side that the GaAs is being formed and to the left at the source side. Typical growth rates of 0.1 to 0.2 microns/minute have been obtained for GaAs and GaP. The only major difficulty here is that the ampoule has to be sealed with as little contamination as possible. Minute quantities of impurities have a large effect on the resulting films.

In the open-tube method a carrier gas such as H_2, HCl or a mixture of both is passed over a heated GaAs or GaP source. The substrate is downstream and at a somewhat lower temperature. At the source the carrier gas receives the compound as a vapor, transports it

downstream and deposits it at the substrate. Gibbons and Prehm (18) indicate that even in this method contamination is a problem and, in fact, certain impurities are transported to and even concentrated in the epitaxial layers.

In sputtering a high, negative potential is applied to the source. A gas such as argon is ionized in the chamber which is at a low vacuum, and the positive gas ions are accelerated to the cathode source. Atoms of the source material are dislodged from their place in the crystal and are subsequently deposited on the surroundings, including the substrate.

Molnar (39) investigated sputtering as a method of growing thin films of GaAs on vitreous silica and polished CaF_2 substrates. The relative location of the substrate in the discharge area and the substrate temperature were found to be the most important factors which influenced the film growth. Predominant (111) orientation was noted when the substrate was located in the positive column and was independent of the substrate temperature. However, for the case where the substrate was located in the Faraday dark space, (111) texture did not appear until substrate temperatures of greater than 500°C were used.

The amount of crystallinity increased with increased

substrate temperature. Above 580°C, however, the film structure deteriorated and this was attributed to the loss of arsenic.

A fairly new idea for growing epitaxial thin films of III-V compounds is the flash-evaporation method. Crushed crystals of the compound semiconductor are fed grain by grain onto a source heater. As the grains hit the heater, they are vaporized. If the grain size and the source-to-substrate distance are chosen properly, successive monatomic layers of first the more volatile element and then the less volatile element are deposited onto the substrate. Theoretically, this would yield a crystal growth of the compound semiconductor in the (111) direction.

Perhaps the most attractive thing about this method is simplicity. The corrosive carrier gases needed for the open-tube vapor-growth method is not required and confined space is not a problem as in the closed-tube vapor-growth method. Also, if large areas of thin-film semiconductor material are required as in large display devices, flash evaporation would be the ideal solution.

II. THEORETICAL DISCUSSION

Crystal Structure

Semiconductors crystallize in a diamond-type structure. In this arrangement the space lattice is a face-centered cubic and the basis associated with each lattice point consists of an atom at 0 0 0 and another at 1/4 1/4 1/4. Here, the position of the atoms are specified in terms of lattice coordinates in which each coordinate is a fraction of the axial length a, b or c, in the direction of the coordinate. Silicon and germanium have this structure.

Compound semiconductors differ slightly in that the basis consists of two different kinds of atoms. A diamond structure can be considered as composed of two face-centered cubic lattices displaced by one-quarter of a body diagonal from each other. If in the compound semiconductor one lattice consists only of one type of atoms and the other consists only of atoms of the other type, the resultant structure is the zinc-blende structure. Compound semiconductors such as GaAs and GaP normally crystallize in this structure.

For GaAs, gallium atoms are located at 0 0 0; 0 1/2 1/2; 1/2 0 1/2 and 1/2 1/2 0, and arsenic atoms are at 1/4 1/4 1/4; 1/4 3/4 3/4; 3/4 1/4 3/4 and

3/4 3/4 1/4. For GaP the phosphorus atoms replace the arsenic atoms. Figure 3 shows the arrangement for GaAs.

As drawn in Figure 3, edge views of planes of gallium atoms only and of arsenic atoms only are seen. The Miller indices for these planes are (111). This is the growth direction of compound semiconductor films produced by the evaporation method.

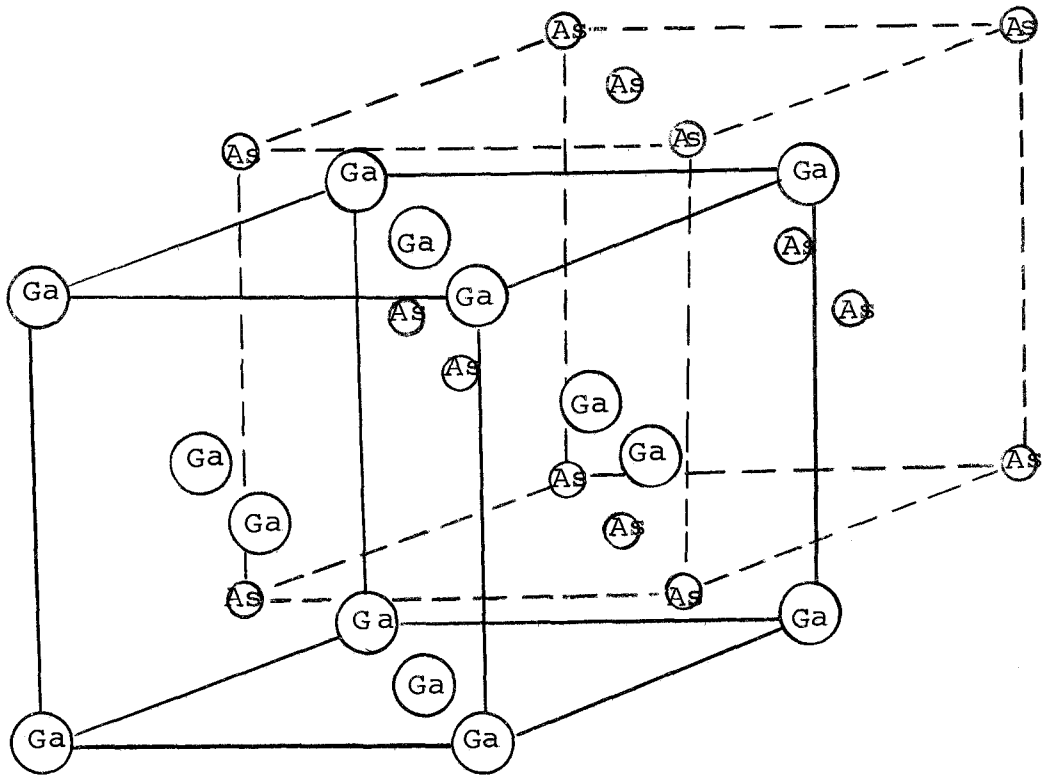

Figure 3. Zinc-blende crystal structure of GaAs.

The lattice constants vary among the different semiconductors since it is dependent on the atomic radii of the constituent atoms. For GaAs the lattice constant is

5.653 Å and for GaP it is 5.450 Å. These are quite near the values for germanium which has a lattice constant of 5.65 Å and silicon with a constant of 5.43 Å.

For solid solutions of III-V semiconductors such as $GaAs_xP_{1-x}$ the lattice constant varies, depending on the value of x. Vegard's law states that the cell dimensions vary linearly as the concentration of the solute (15). It was shown later by Vegard, however, that over the whole range this linear relationship was correct only to the first approximation.

The extent of solid solution is limited by geometrical considerations. These include the relative sizes of the atoms concerned and the amount of distortion a lattice can tolerate without change in structure. Hume-Rothery, Mabbott and Channel-Evans (24) showed that for extended solid solutions a maximum difference of 15% in atomic radii can be tolerated. Phosphide-arsenide systems have been shown to be completely miscible by Müller and Richards (41). These systems follow Vegard's law very closely. Figure 4 shows the lattice constant versus composition for the GaAs - GaP system.

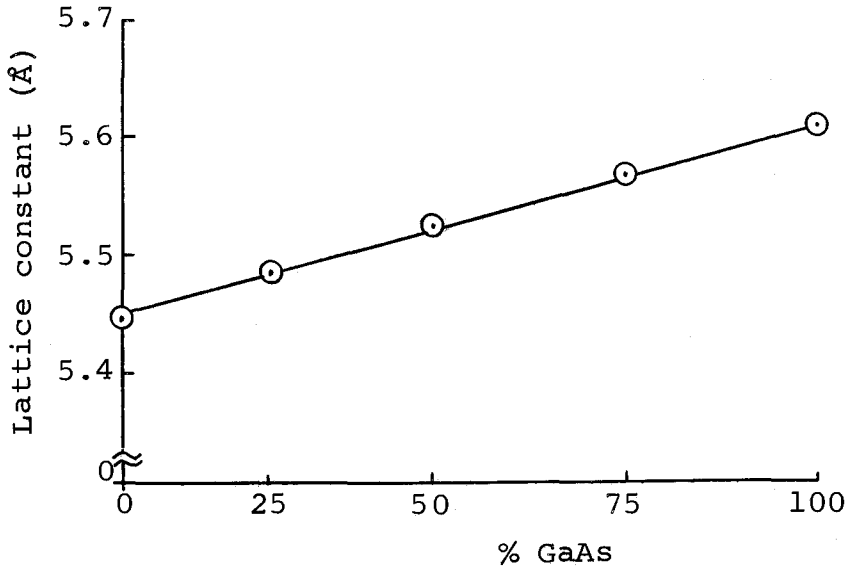

Figure 4. Lattice constants for various compositions of GaAs-GaP systems (40).

Crystal Growth

The nature of the substrate, the temperature of the substrate, the rate of deposition and the residual gas pressure during deposition are four factors which are known to be important in epitaxial crystal growth. The term epitaxial growth is used here in the broad sense of the term. That is, epitaxial growth is understood to be the formation of a crystal with each crystal layer growing with the same orientation as the layer beneath. The original meaning of the term epitaxy, as used by Royer, referred to oriented crystallization on foreign

substrates.

In the crystal pulling technique, the "seed" crystal determines to a large extent the nature of the resulting crystal. A single-crystal seed is required for a single-crystal rod. Similarly, the substrate is the seed for growing vapor-deposited films and should be single crystalline if single-crystal film growth is desired.

Since the substrate must be heated in the deposition process, the coefficients of thermal expansion of the film and the substrate should be similar. If there is too great a variance, strains will develop during cooling and may have an adverse effect on the properties of the film.

In epitaxial growth the film grows with the same orientation as the substrate. Therefore, in the nucleation phase it is desirable to have the crystal structure of the substrate like that of the film to be grown. Although this is desirable, it is not necessary, as single-crystal films of silicon and germanium have been grown on substrates with appreciably different crystal parameters (34, 36).

Besides the bulk nature of the substrate, the condition of the deposition surface is also important. For instance, scratches on the surface form centers of high growth rates which result in polycrystalline films.

Smooth surfaces result in films with much less multiphase areas.

Surface cleaning determines to a large extent the nature of the deposition surface. To deposit the most durable and adherent epitaxial layer, the substrate surface must be free from contaminant films such as grease, adsorbed water, etc. Several methods are available for cleaning substrate surfaces. Among these are chemical cleaning, vacuum baking and ion bombardment.

Chemical cleaning is effective in removing gross surface contaminants. However, a cleaned surface rapidly becomes contaminated when exposed for even a short period to normal atmosphere. Since chemical cleaning is normally done outside the vacuum system, contamination occurs during the transfer to the system.

Vacuum baking has the advantage that contamination after cleaning can be prevented since the process is carried out in a vacuum. It is most effective in removing absorbed gases. However, grease films are not removed very effectively. Holland (27) notes that a finger-mark on the surface of a glass specimen was effectively removed by ionic bombardment, but baking left a stain on the glass surface. Also for some compounds like GaAs high temperatures tend to outgas the more volatile component, thus damaging the crystal

surface.

Ionic bombardment is a very important method of surface cleaning. It can remove surface films not consistently cleaned by other methods. Surfaces prepared by this method have been shown to be extremely satisfactory as witnessed in the aluminizing of glass surfaces.

The cleaning mechanism for ion bombardment is very complex. Generally, cleaning is accomplished by chemical reactions between adsorbed layers and active gases and sputtering of contaminant films from the substrate in a low-pressure glow discharge.

The type of discharge which occurs at low pressures depends on the gas pressure, the discharge path length, the electrode geometry and the value of applied voltage. The desirable area of operation is the region called "abnormal glow discharge" (27). In this region, the voltage and the cathode dark space are large enough for cleaning purposes.

Surface contaminants are removed by chemical reactions due to the presence of either oxidizing or reducing gases in the discharge. For example, hydrocarbons are decomposed by bombardment and if there is oxygen in the residual gas, the carbon constituent is removed as CO.

In the sputtering mechanisms the ions remove surface

contaminants by dislodging them by actual collision. The ions are formed by collision of electrons and gas molecules in the positive column and are accelerated toward the cathode. It is necessary then to have a large cathode dark space so that electrons can be accelerated sufficiently to ionize the gas molecules. The high velocity of the ions impinging on the surface has some damaging effect on the surface. This would, of course, affect the perfection of the deposited film.

The geometry and materials used in the electron bombardment apparatus is also of importance. Due to the sputtering of all surfaces being bombarded, the surface being cleaned may be contaminated by these sputtered materials. Aluminum is known to have a low sputtering rate and is thus a suitable electrode material for the bombardment apparatus.

The best cleaning method is probably a combination of these individual techniques. The situation will dictate to what extent each should be used.

The temperature of the substrate has three important effects. These are the critical size and rate of formation of the nuclei, the mobility of the adsorbed atoms and the annealing of defects in the condensed films. At low temperatures the rate of nucleation is large and many crystal centers are formed. The result

is a highly imperfect or polycrystalline film. Higher temperatures result in less nucleation centers and, hence, a less polycrystalline film. At too high a temperature, however, rod-shaped or faceted crystals result instead of a uniform film (19).

The proper substrate temperature is not an inherent property of the substrate but depends on numerous factors including rate of deposition. Consider a vapor flux of density, n_+, impinging on a heated substrate. Some of the particles landing on the substrate will be immediately reflected, but most will be absorbed and temporarily held to the surface. These particles gain a certain mobility, depending on the substrate temperature and the energy of the position change, Φ_n. If they are not re-emitted into the vapor phase, they soon reach growth centers of high bonding energy. The particles are then held strongly to the substrate and the possibility of subsequent re-emission is drastically reduced. Figure 5 shows the relative energy variation along a linear path. Φ_c is the condensation energy while Φ_k is the bonding energy of a growth center.

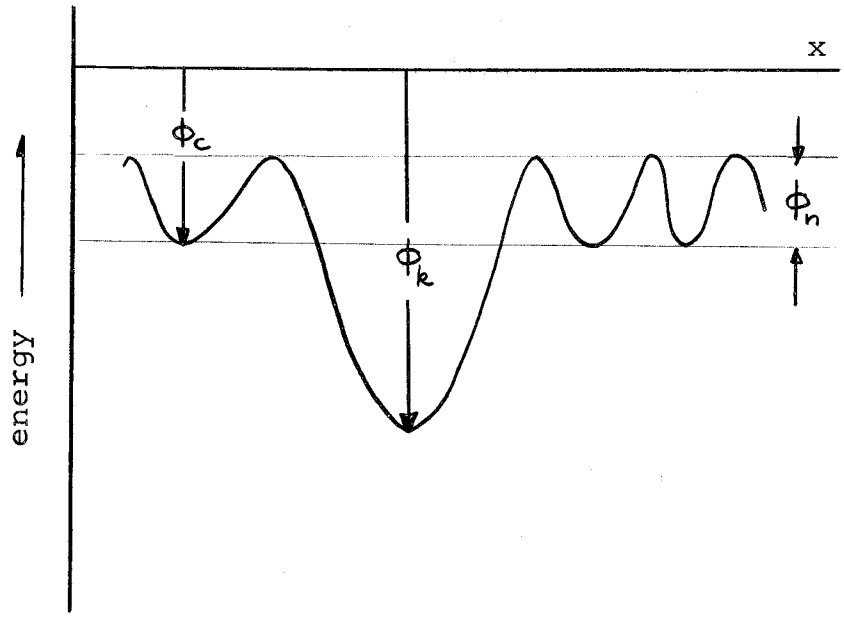

Figure 5. Relative energy variation along a linear path on a substrate surface.

The various positions a particle can take on a crystal are shown in Figure 6. Each location has a chacteristic bonding energy which controls the subsequent motion of the particle. In position e, for instance, the particle is held loosely, and consequently the probability of the particle remaining there is small. At b, however, the bonding energy is much greater and so the particle remains there for longer periods of time. The chances for crystal growth is thus increased and b is then a practical growth center.

Growth centers exist at surface imperfections of the substrate. These nucleation points are necessary

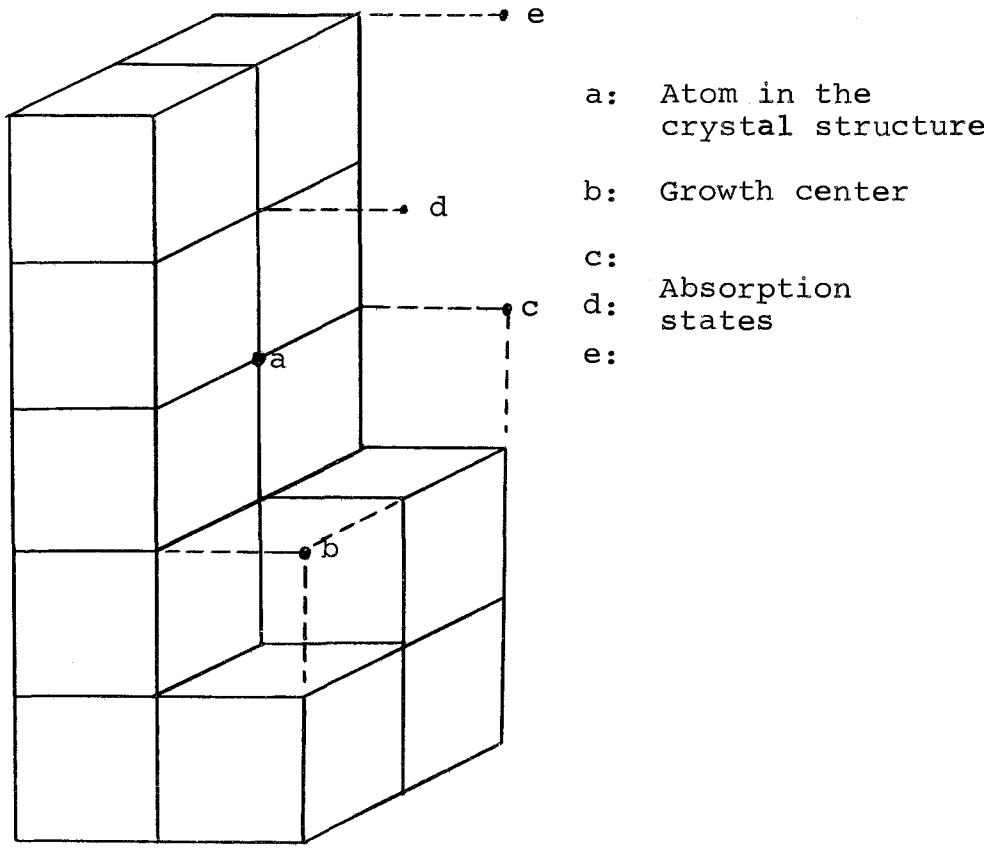

Figure 6. Positions of different bonding energies in a crystal lattice.

to insure crystal growth at a practical rate. The theory of crystal growth due to Gibbs, Volmer and others predicts that for a perfect crystal face a supersaturation (pressure/equilibrium vapor pressure) of the order of 10 is necessary to nucleate new crystals (31). Supersaturation of the order of 5 is required to form liquid drops and 1.5 to form a monolayer. Surface imperfections aid the crystallization phenomena to such an

extent that low supersaturation is sufficient for practical growth rates.

The condensation coefficient (50) is given by

$$a = \frac{n_+ - n_-}{n_+} = 1 - (\text{const})\, e^{-\frac{\Phi_c}{kT_k}}$$

Here, n_+ is the impinging flux density (particles per unit time and unit surface), n_- is the reflected flux density, Φ_c is the energy of absorption and T_k is the substrate temperature. When T_k exceeds a certain value, T_g, as shown in Figure 7, n_+ becomes less than n_- and no condensation takes place.

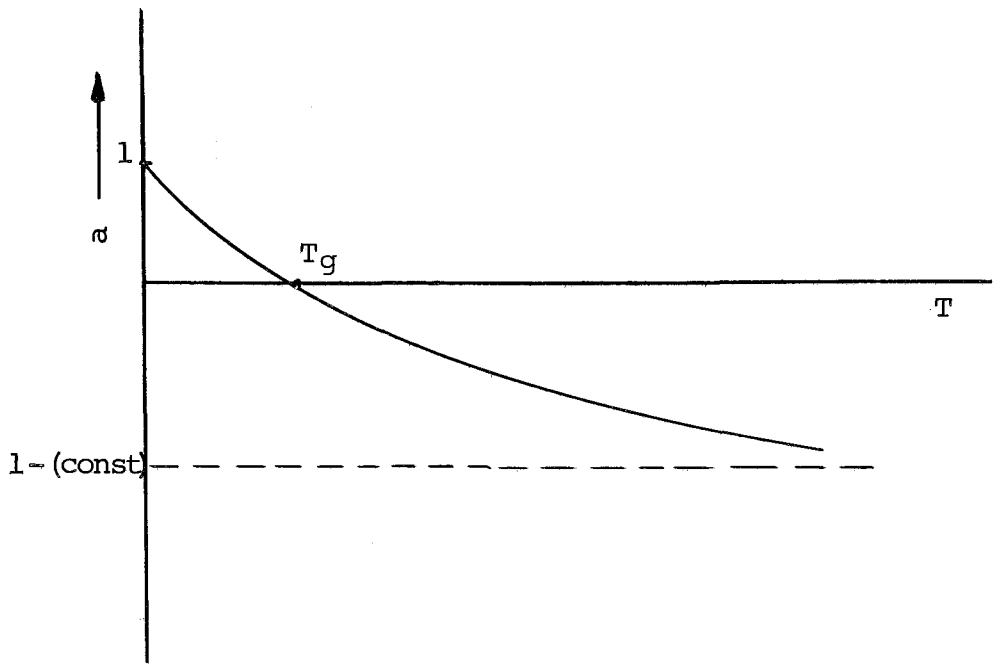

Figure 7. Variation of the condensation coefficient with substrate temperature.

If two different vapor fluxes of molecules impinge on a surface, the interaction between the two has to be considered. Since for normal deposition the flux densities of the impinging molecules fall between 10^{14} to 10^{18} particles/sec-cm^2, reaction in the vapor need not be considered. Gunther (52) notes that on the surface the intermolecular reactions can cause the condensation coefficient to increase for both molecules.

The evaporated films become less perfect as the rate of deposition is increased. The reason for this is not yet understood, but if the rate of deposition is too high, amorphous films result. As the rate of deposition is decreased, the films become more and more crystalline until finally at low enough rates, total crystallinity can be expected.

One of the possible mechanisms contributing to the imperfection at high growth rates is the increased rate of nucleation. The resultant crystal is necessarily polycrystalline at best and the probability of amorphous growth is high.

Another mechanism that may enter in is the decrease in transit time. A molecule at a condensation site may become trapped there by the molecules arriving after it. If the condensation site is not the proper place for the trapped molecule in the final lattice, a defect results.

A high rate of deposition increases the possibility of this event occurring and hence increases the number of defects formed in the crystal.

Contamination of the film by electrically important residual gas molecules can change the properties of the films. For instance, oxygen is known to form a deep donor level in GaAs and even at low concentrations tends to make the crystal resistivity high. Low vacuum depositions minimize this effect, and pressures of 10^{-6} Torr or lower should be used to alleviate the situation.

The Flash-Evaporation Method

For flash-evaporation crystal growth, the desired particle flux is such that alternating monolayers of the component elements are deposited on the substrate. This can be assured if the feeding mechanism drops one grain at a time slowly enough so that the first grain is totally vaporized before the next arrives. Experimentally, this is difficult to achieve. Therefore, a more rapid delivery is used in which many more grains of the evaporant arrive before the first one is fully vaporized. At any time, however, the evaporator contains the same number of grains at various stages of decomposition. At equilibrium, then, the composition of the vapor flux remains constant. Since there is no net accumulation of

material in the evaporator, this flux must have the same composition as the original evaporant.

In practice, the stream of grains delivered to the heater varies so that the amount of material in the heater does not remain constant. Hence, the composition of the vapor flux changes. This is best seen in the extreme case where the powder flow is abruptly stopped and, after an interval of time, started again. The flux composition will be richer in the less volatile material just after the flow has stopped. In the initial phases of the subsequent evaporation, the composition will be much richer in the more volatile component. The result is that more than a monolayer of one component could be deposited onto the substrate and cause difficulties in attaining the proper stoichiometry.

This difficulty is somewhat overcome by the fact that free energy considerations favor the proper stoichiometry. The particles evaporated onto the substrate have sufficient mobility to find a proper place in the lattice if the temperature is high enough. However, the maximum temperature limit is set by the relation for condensation coefficient, and, as noted by Paparoditas (52) in his work on compound evaporation, the annealing process must be completed before a critical thickness of cover material is deposited over the layer.

The size of the evaporant particles determines to a large extent the source-to-substrate distance. This is a consequence of the requirement that monolayers of gallium and arsenic or phosphorus are to be alternately deposited on the substrate.

The thickness of a film evaporated from a small area source to a parallel plane receiver is given by

$$t = \frac{m}{\pi\rho} \frac{\cos^2\Theta}{R^2}$$

where R is the source-to-substrate distance, Θ is the angle between the normal and the line joining the source and the point of deposition and m/ρ is the volume of the evaporated material. Assuming that the evaporant particles are spherical, the volume is given by

$$v = \frac{4}{3}\pi r^3$$

where r is the radius of the spherical volume. Substituting this in the previous equation and solving for R

$$R = \left(\frac{4}{3}\frac{r^3\cos^2\Theta}{t}\right)^{1/2}$$

If R is large compared to the radius of the substrate surface, Θ can be taken as 90°. This simplifies the equation for R to

$$R = \left(\frac{4}{3}\frac{r^3}{t}\right)^{1/2}.$$

The lattice constant of GaAs and GaP is about 5.5 Å. This means that the thickness of a monolayer, which is

1/6 of the diagonal of the unit cell, is approximately 1.6 Å. Substituting this value for t in the above equation, the relation between R and r is given by

$$R = 9150\ r^{3/2}.$$

It should be noted that the value for r must be in centimeters in order to use the last equation. The value for R will then be also given in centimeters.

As an example, consider the particles that pass through a 100 mesh screen. The maximum diameter of these particles is 1.8×10^{-2} centimeters. Using this value for r, R is about 7.8 centimeters or 3.1 inches. The minimum source-to-substrate distance, then, should not be less than this value if successive monolayers are to be deposited.

Optical Properties of Semiconductors

The width of a band gap of a semiconductor can be determined by optical measurements. Consider the theory of light dispersion in a solid. The contributions from the bound electrons and the free electrons are usually considered separately. In a non-conducting dielectric the former dominates while in metals the free electron contribution is more important. For semiconductors both are important. At high energies intense absorption due to bound electrons is seen. The free electron contribution is seen at low energies. In Figure 8 the

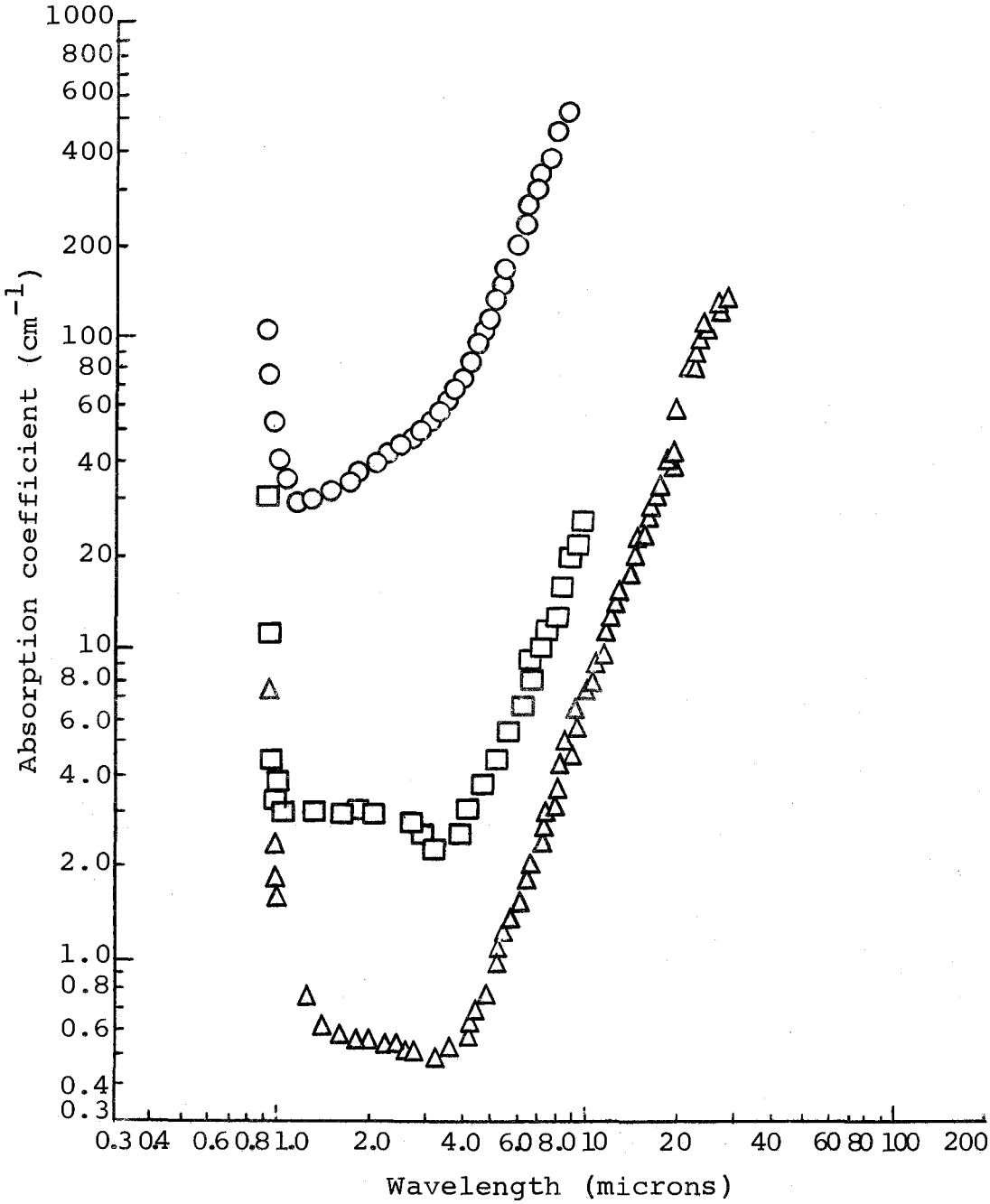

Figure 8. Absorption coefficient of N-type GaAs for three samples of different doping. (After Spitzer and Whelan)

absorption coefficient versus wavelength for several samples of GaAs is plotted, showing the two absorption edges discussed above.

The shape of the absorption edge between the high frequencies and absorption minimum is determined by the nature of the optical transitions between the bottom of the conduction band and the top of the valence band. In a direct transition the absorption coefficient (40) is given by

$$K \sim \left(\frac{h}{2\pi}\,\omega - \Delta E\right)^{\gamma}$$

where ΔE is the smallest difference between the initial and final states. γ has the value of 1/2 for allowed transitions and 3/2 for forbidden transitions. GaAs is a direct-transition semiconductor.

In an indirect-transition semiconductor such as GaP, the absorption constant is slightly more complicated as transitions are possible only with phonon cooperation. The absorption constant is then composed of two terms, the direct transition of an electron and an absorption or an emission of a phonon.

The energy gap can be determined by observing the absorption with respect to incident optical energy. As the energy of the incident beam decreases, a point is reached where the energy is not sufficient to promote electrons from the valence band to the conduction band.

An abrupt decrease in absorption is noted at this point corresponding to the band gap.

The experimental edge is not infinitely steep due to several factors. Since there is a need for a unique value of E_g from the optical data to compare with values obtained by other means, several definitions have been proposed. Moss (40) defines the band gap energy as that value where the absorption constant is one-half its maximum value. An alternate definition is to take the band gap energy as the point where the slope of the absorption coefficient is maximum.

Electrical Properties of Semiconductors

According to the band theory of solids electrons from the valence band are excited into the conduction band at any temperature above absolute zero. The higher the temperature the more electrons excited into the conduction band. In an intrinsic semiconductor crystal this results in an increase in conductivity as temperature increases. This is in contrast to most metals in which conductivity decreases with increasing temperature.

The energy gap can be determined from the conductivity-temperature data. Since the number of electrons excited into the conduction band, n, is proportional to $e^{-\frac{cEg}{T}}$ where c is a constant, and since conductivity is

proportional to n, $\ln\sigma = -\frac{E_g}{T} + K$ where K is another constant. The plot of $\ln\sigma$ versus 1/T is a straight line whose slope is equal in magnitude to the band gap of the semiconductor.

Impurities introduced in the semiconductor crystal change the band structure by introducing allowed levels in the forbidden gap. If the impurity is n-type, a band of electrons close to the conduction is formed. These electrons are easily excited into the conduction band by thermal energy and the increase in conduction electrons increase conductivity. A tellurium atom substitutionally introduced in an arsenic location in GaAs provides a donor of this type.

If the impurity is p-type, an empty band is introduced close to the valence band. Thermal energy excites electrons from the valence band into the impurity band and the result is an increase in hole concentration. This also results in an increase in conductivity since the carrier concentration is increased. A zinc atom introduced substitutionally in place of a gallium atom in the GaAs crystal structure forms an acceptor of this type.

The temperature-versus-conductivity curve is altered by the addition of the impurity levels. Starting from absolute zero the slope of the curve is

determined by the impurity ionization energy level and not the band gap. As the temperature is increased, a point is reached where all the impurities are ionized and the conductivity levels off. With further increase in temperature the electrons from the valence band which have been excited all along begin to dominate and the conductivity increases again as determined by the band gap energy. Figure 9 shows the conductivity-versus-temperature curve for GaAs as done by Folberth and Weiss (16).

When a conductor is placed in a magnetic field perpendicular to the flow of the charged carriers in the conductor, a voltage results which is perpendicular to both the magnetic field and the direction of charge flow. The resulting voltage is known as the Hall voltage and is the result of the deflection of the moving charge due to the magnetic field. Mobility and carrier type can be determined from the Hall data.

The magnitude of the Hall voltage can be found by first considering the Lorentz force on a charged carrier is

$$\overline{F} = e\left(\overline{E} + \frac{1}{e}\,\overline{v} \times \overline{H}\right)$$

For Hall voltage in the y direction, magnetic field in the z direction and motion of charged carriers in the x direction,

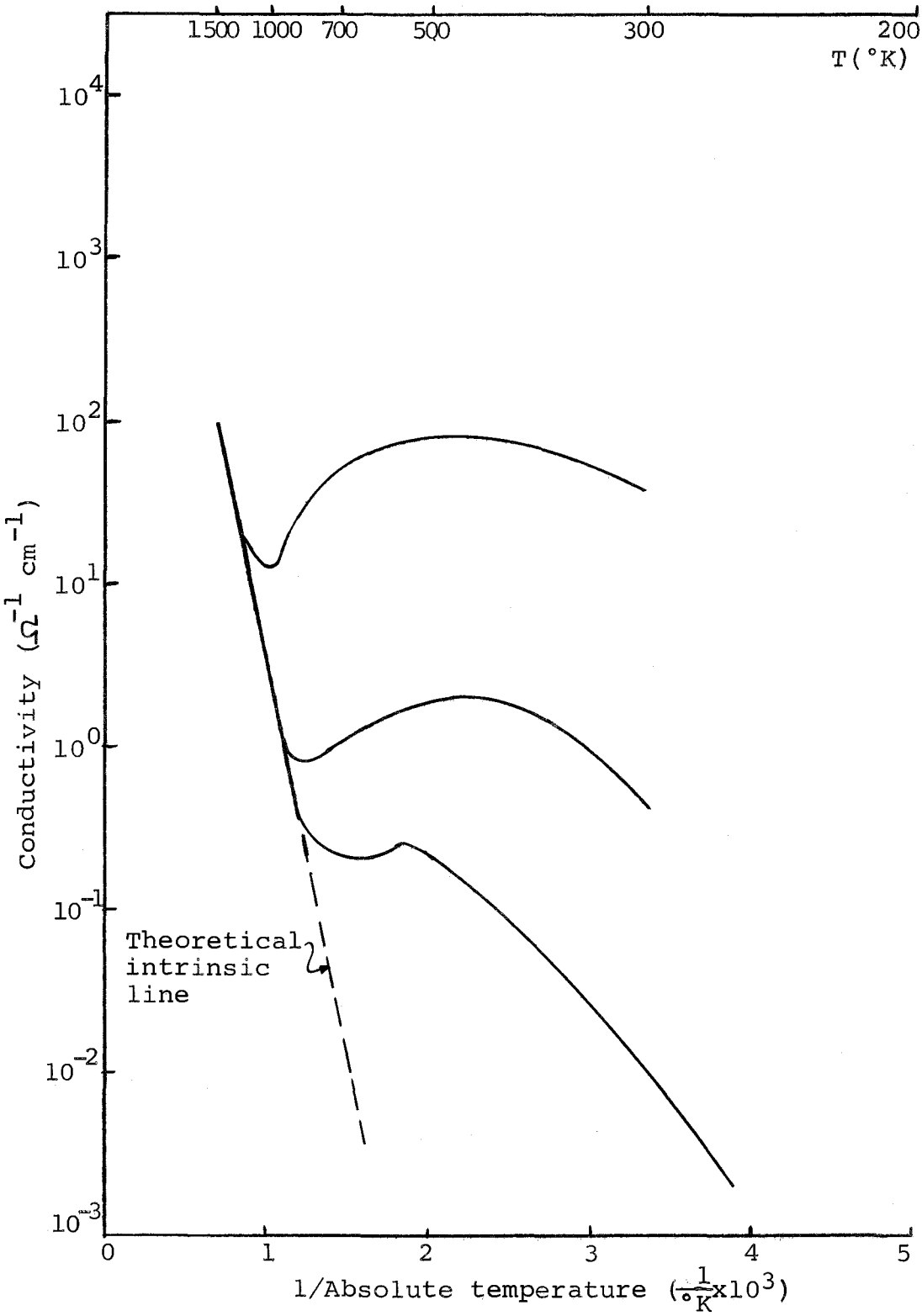

Figure 9. Temperature dependence of conductance for GaAs samples of different doping. (From Folbert and Weiss)

$$V_H = \frac{R_H I H_z}{W x 10^8}$$

where R_H = Hall constant. But

$$R_H = \frac{\mu_H}{\sigma} \quad .$$

So that

$$\mu_H = \frac{V_H W \sigma x 10^8}{I H_z} \quad .$$

Electroluminescence

Radiative recombination in semiconductors results from the combining of majority carriers with excess minority carriers. These minority carriers can be created in several ways. They may be excited by irradiation with photons, in which case the resulting luminescence is known as photoluminescence. They may also be excited by irradiation with electrons. This type of luminescence is called cathodoluminescence. If the minority carriers are created by injection across a potential barrier, electroluminescent radiation results.

The potential barrier for radiative recombination takes several forms. The most common is a pn junction. Radiative recombination from this type of junction has been noted by many workers in GaP and GaAs among other

materials. Starkiewicz and Allen (48) have observed two types of electroluminescence in alloyed GaP diodes in the forward-biased mode. They note that for zinc-doped GaP green emission was seen and for zinc and oxygen doping there was red emission. Oxygen doping alone did not give off any emission.

Orange electroluminescence has been observed in reverse-biased pn junctions of GaP. Logan and Chynoweth (38) have attributed this to band-to-band recombination of "hot" carriers. Reverse-bias electroluminescence was also noted by Gershenzon and Mikulyak (17), the spectral curve of which is shown in Figure 10. The spectra of these reverse-bias diodes were the same, irrespective of whether emission occurred during avalanche breakdown (microplasma), zener breakdown or prebreakdown. This implies that although the mechanisms for creation of excess minority carriers is different, the radiative recombination step is the same for reverse-bias emission. It should also be noted that the peak for the spectral curve occurs below the band gap energy. This conflicts with the results of Logan and Chenoweth. Gershenzon and Mikulyak note, however, that the structure they used may have been highly absorbent of photons with energies above the band gap.

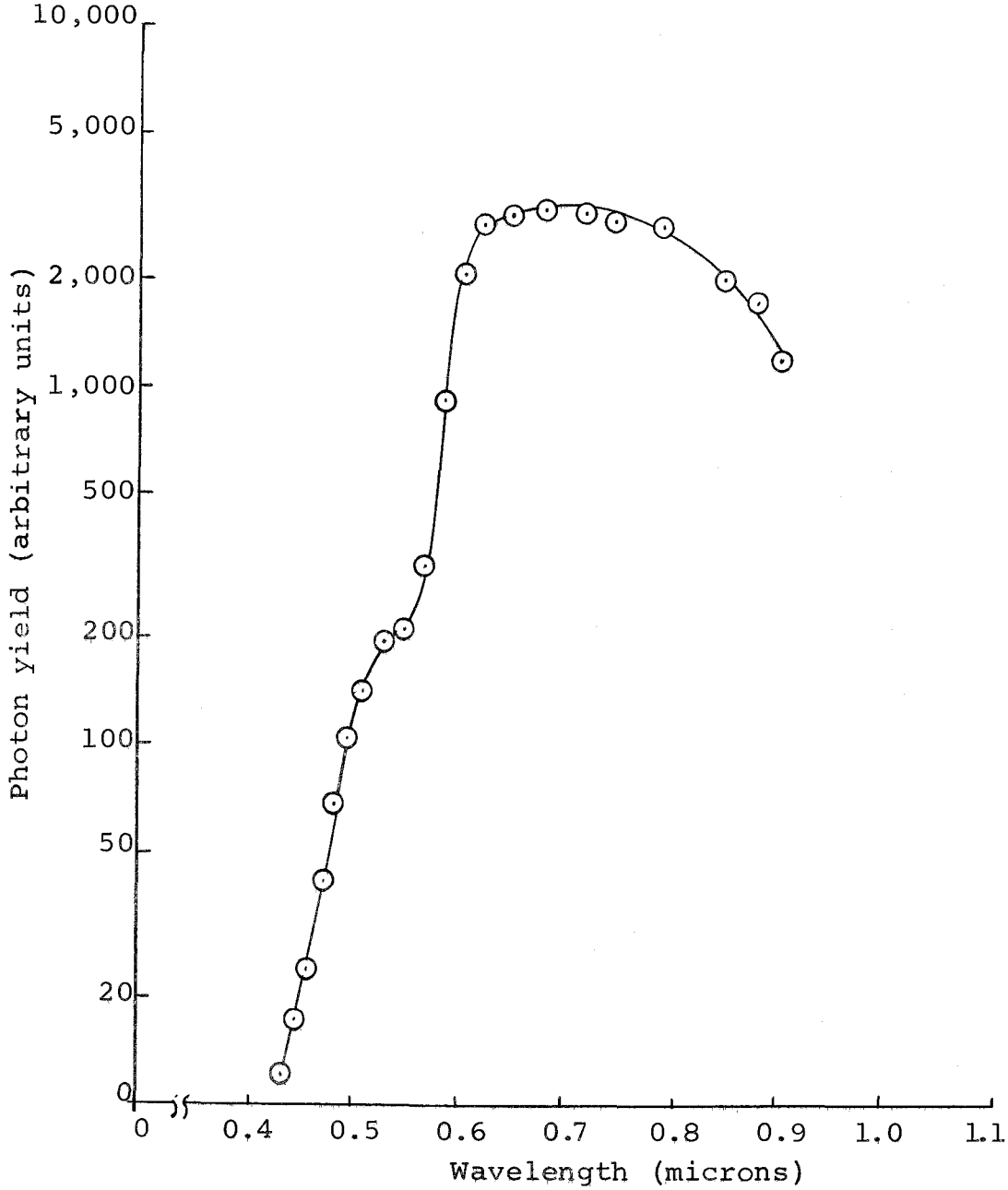

Figure 10. Electroluminescent spectral response of a reverse-biased alloyed GaP diode at 300°K.

Metal-semiconductor (MS) junctions, metal-insulator-semiconductor (MIS) junctions and heterojunctions also form potential barriers. Eastman, et al. (12) have observed electroluminescence in MS and MIS junctions using p-type ZnTe as the semiconductor. For the MS junction a narrow spectral peak at 0.5375 microns was observed. Since avalanche multiplication usually results in a broad spectral band, an alternate model was presented. Tunnelling effects were postulated as the most important mechanism in their model and the subsequent recombination theoretically predicts a narrow spectral band.

Not all recombination processes are radiative, however. In the Auger process band-to-band recombination takes place, but instead of a photon being emitted, an electron is promoted to one of the higher lying energy levels in the conduction band. The electron energy then decays in a nonradiative manner since a continuous distribution of states exists to a lower, stable level. Other nonradiative processes include recombination at dislocations, crystal interfaces and other defects. These processes compete with the radiative ones and the efficiency of luminescence is highly dependent on which processes are favored.

III. EXPERIMENTAL APPARATUS AND PROCEDURE

The Pumping System

The apparatus used to develop the vacuum for the evaporations consisted of a 17.7 CFM Edwards Mechanical Pump as the roughing system and a Varian Titanium Sublimation pump and a Varian Sputter-Ion pump for the low pressure system. The vacuum chamber consisted of an 18-inch diameter by 30-inch high Pyrex bell jar and a stainless steel staging platform. Figure 11 illustrates the relative locations of the various parts of the system.

An oil sealing device, consisting basically of a spring-loaded washer which seals the mechanical system, minimizes oil vapor leaks back into the chamber. A molecular sieve, located between the pump and the chamber, also minimizes oil vapor leaks.

The Varian Sputter-Ion system used for low-pressure pumping has the capability of evacuating chambers to below 10^{-11} Torr. Since it does not contain any pump fluids or moving parts, it is inherently clean. The pump traps or removes gas particles through the following processes:

1. Gas ionization
2. Titanium sputtering

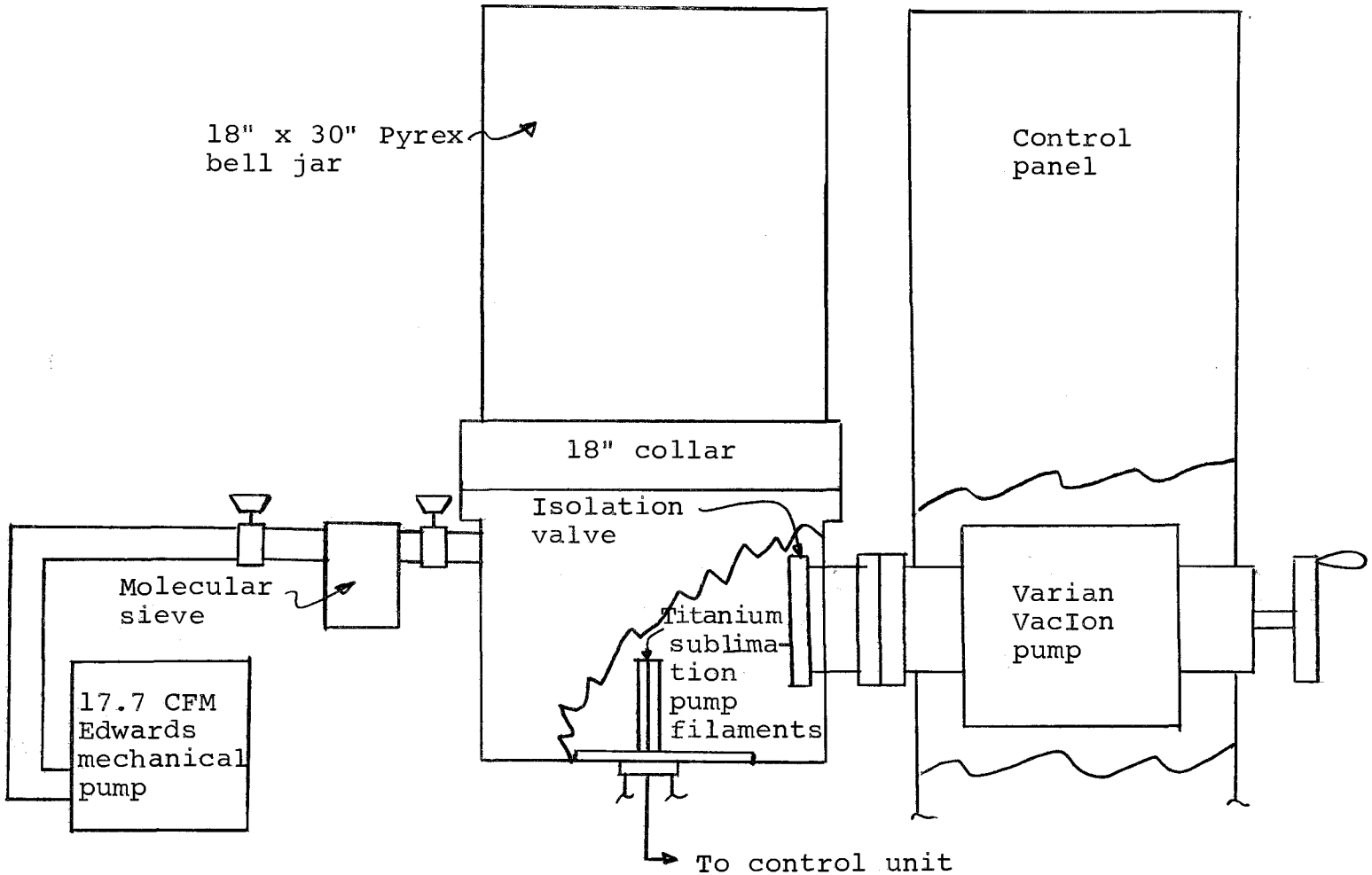

Figure 11. Arrangement of vacuum system components.

3. Chemical combination with titanium for active gases
4. Ion burial for heavy noble gases
5. Ion burial and diffusion into cathode plates for hydrogen and helium

A schematic of the Sputter-Ion pump is shown in Figure 12.

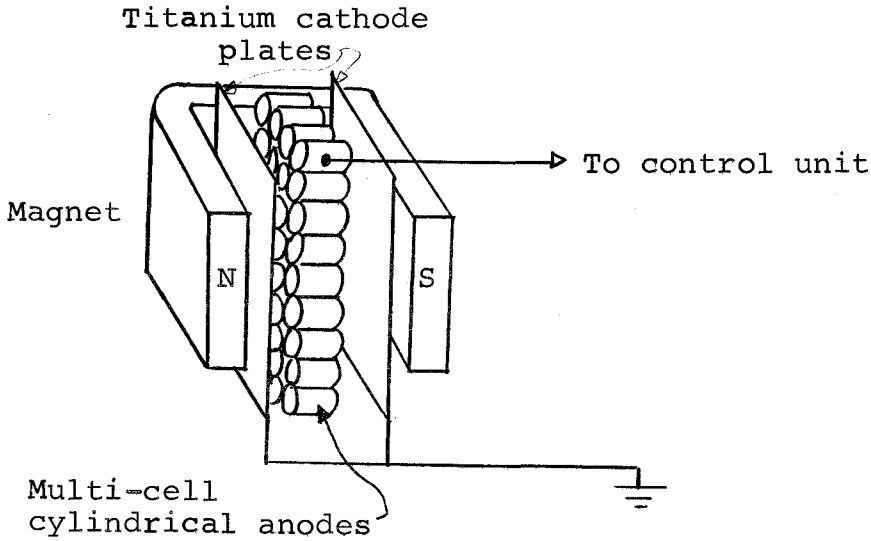

Figure 12. Internal structure of the Varian Sputter-Ion pump.

The titanium sublimation pump works on the principle that freshly deposited titanium forms stable, solid compounds with the gas molecules that strike the gettering surface. The titanium is sublimed from a special filament through resistance heating. For the

systems used, the lower portion of the staging platform served as the gettering surface.

Pumping speed is maximum at low pressures since the pumping speed is maximum when the entire gettering surface is covered with fresh titanium. In this pressure range the pumping speed is only limited by the speed at which the gas molecules enter the pump from the chamber. At higher pressures, the pumping speed is determined by the rate of titanium deposition.

Source Heater

Several requirements had to be met by the evaporation source heater used. The geometry had to be such that the entrance for the falling particles from the feeder be large enough to capture most of the falling particles, and the source had to be deep enough so that the evaporating particles did not escape before vaporizing. Yet the total size of the heater had to be small enough so that excess power was not dissipated. Large power dissipation in the vacuum system resulted in rapid rise of pressure which conflicted with the requirement of making the depositions at the lowest possible pressures.

Various types of geometries were considered. Figure 13 shows the three basic types considered.

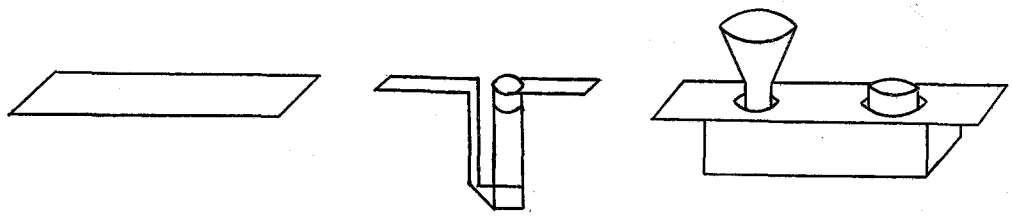

a) flat strip b) deep-cup c) horizontal

Figure 13. The three basic types of source heaters used.

The flat strip of tantalum offered the simplest geometry and the least heat problems. However, most of the particles falling on the heater did not vaporize completely. Instead, much of it was scattered in all directions, some of it towards the substrate. Those that landed and adhered to the substrate masked those areas from subsequent film growth. These particles were later cleaned off and removal of this excess material revealed numerous pits in the film.

The deep-cup geometry offered fairly low power dissipation, but the entrance for the evaporant particles was relatively small and much of the falling evaporant did not fall into the evaporator. Increase in entrance diameter resulted in an increase in power, so improvement in this manner was limited.

The vapor flux leaving the cup tended to "blow away" the incoming lighter particles so that even with less

unvaporized particles impinging on the substrate, the films grown using the deep-cup source had an undesirably large number of pits. It was also noted that the higher the source temperature, the larger the number of unvaporized particles leaving the source and hence the greater the number of pits in the film.

The horizontal source had a major disadvantage in that, of the three, it required the largest amount of power. Another disadvantage was that the entrance port was small. Part of this problem was reduced by the funnel at the top of the entrance column, but this caused scattering as the particles fell through the column. Towards the hotter part of the column the source material hitting the walls formed a sticky substance, probably metallic gallium, and eventually closed the opening.

Despite the disadvantages, the horizontal source was used in a major portion of the experiment because the resulting film had very few pits. It also allowed placing the substrate very close to the source which increased the efficiency of the system. That is, thicker films could be grown for a given amount of source material.

Substrate Heater

The substrate heaters used in this study consisted of a ceramic disc heater and a resistance-heated tubular oven. Both proved satisfactory in accomplishing the objective.

The ceramic disc heater shown in Figure 14 consisted of a tantalum filament threaded through a ceramic support. The thermocouple was attached to the face of the heater and the substrate was held in place using a molybdenum clip. The maximum temperature obtainable by this heater was about 675°C.

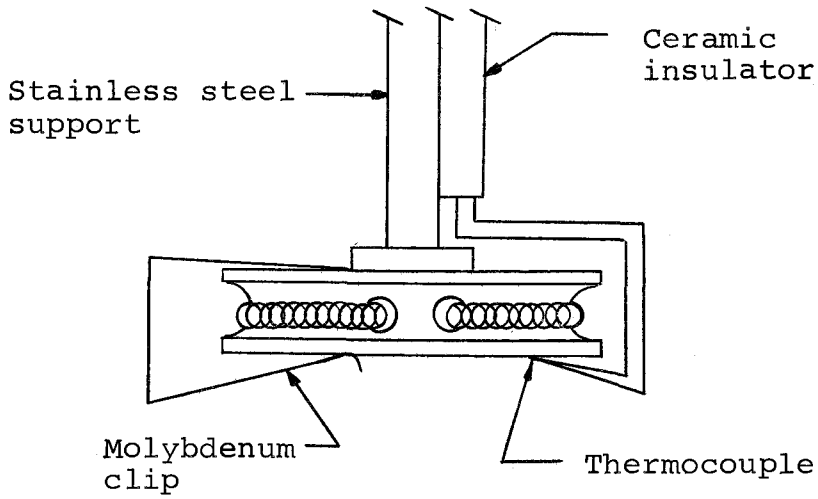

Figure 14. Ceramic disc heater used for substrate heating.

Figure 15 shows the tubular oven used. Nichrome wire 50 mils in diameter was used as the heating element. Aluminum oxide placed between the outer stainless steel heat shield and the ceramic tube increased the efficiency of the system. Outgassing, particularly if the system was left at atmospheric pressure for any appreciable time, was a problem because of the affinity for gases of the AlO_2.

The ceramic disc heater had the advantage that the heating and cooling times were much less. This was somewhat overcome when using the tubular oven by using a device which lifted and lowered the substrate holder assembly in and out of the oven after the oven had reached the desired temperature. The length of time involved in heating or cooling, however, did not result in obvious differences in the films grown.

Particle Feed System

A method of feeding the evaporant particles in a uniform manner to the source heater was desired. Initially, a trough with a circular reservoir was mounted on a half-inch feedthrough. A solenoid was placed on the external portion of the feedthrough and the source material was fed down the trough by the resulting vibration. The powder feed rate was fairly well controlled

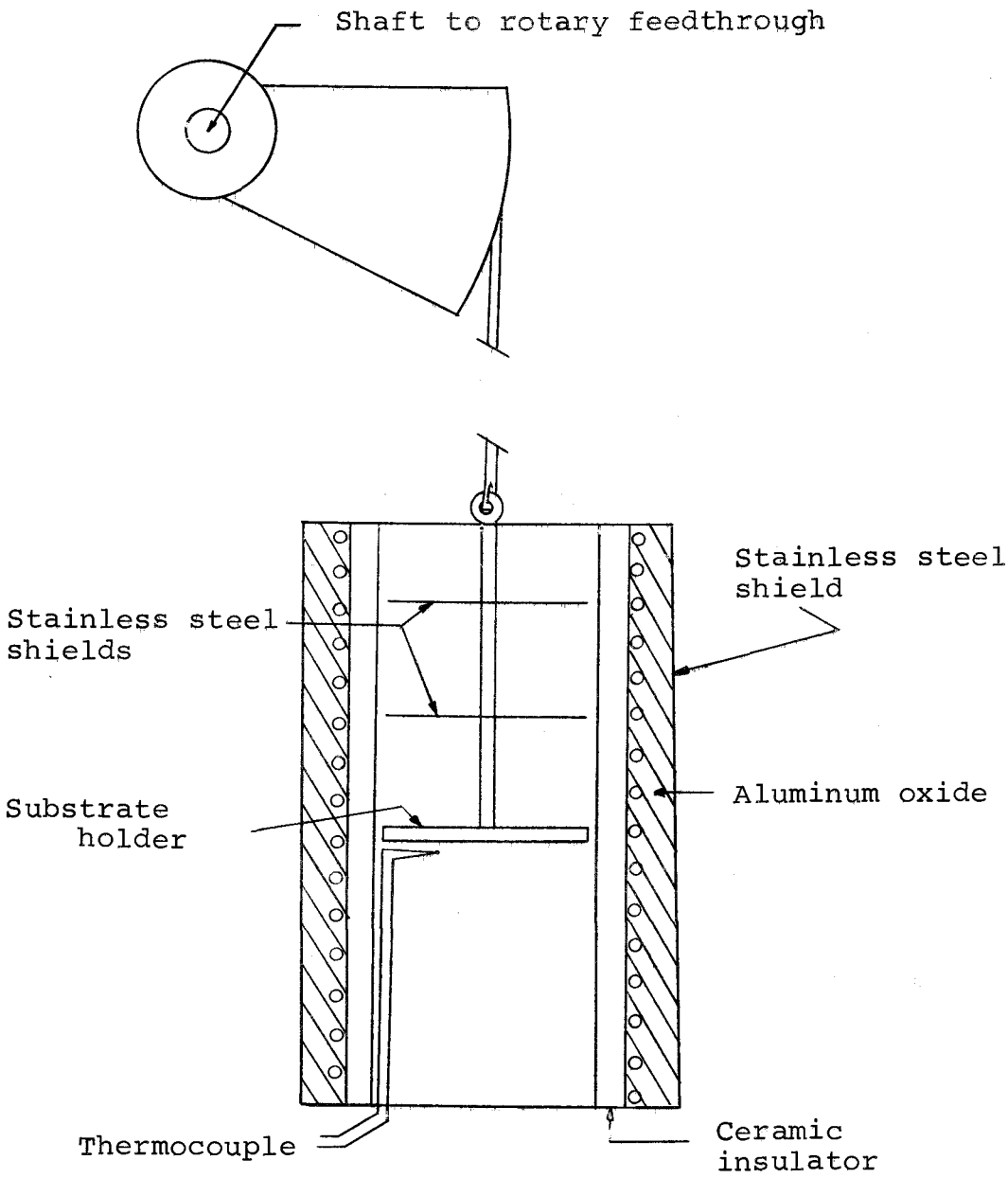

Figure 15. Tubular oven used as the substrate heater.

for fast evaporations but was not satisfactory for slower rates. At slower rates the evaporant particles tended to bunch up as they progressed down the trough.

An alternate method using the same setup was to vibrate the feeder manually. This worked fairly well for short periods of time but was unworkable for longer times.

Another method, which was ultimately adopted for the experiment, was to use a Bendix-Balzer vibratory feed system. Although the powder-feed rate depended on the size of the particles, control of the feed rate was good. Larger particles tended to be dropped before the smaller ones.

The rate of feed of the evaporant material was a major factor in controlling the rate of film deposition but other effects also entered in. As was pointed out in the heater-filament section, the amount of powder evaporation depended quite heavily on the heater geometry and the temperature of the heater. These effects coupled with the source-to-substrate distance and the substrate temperature determined the rate of film deposition.

Substrate Preparation

Substrates of GaAs, both n- and p-types, germanium and sapphire were used in this experiment. Preparation of the GaAs substrates consisted of first mechanically polishing the wafers using a 1:20 bleach:water etch, washing in acetone, rinsing in deionized water and air drying. Some were etched with a solution of 1:1:2 $HCl:HNO_3:H_2O$ instead of mechanically polishing them. The mechanically polished wafers were more desirable as it allowed thickness measurements by the interferometer method.

The germanium wafers were polished with 0.5 micron alumina and then etched in CP4. An acetone rinse, deionized water rinse and air-drying followed. The sapphire wafers were cleaned in acetone in an ultrasonic cleaner for a minimum of five minutes, washed in deionized water and air dried.

In most cases, the wafers were subsequently cleaned by ion bombardment in the evaporation chamber. Nitrogen was used as the ionization atmosphere and about 1000 volts was applied at 10 to 15 microns pressure. The bombardment time varied from five minutes to 30 minutes.

For the glass and ceramic substrates which were used to a limited extent, the preparation was essentially the same as that for the sapphire substrates.

Source Material Preparation

There were three sizes of evaporants used in this study. These were prepared by crushing GaAs and GaP wafers with a mortar and pestle. The first consisted of grains between 100 and 200 mesh while the second consisted of the powder that passed through the 200 mesh screen. The third was prepared by passing the crushed material through a 100 mesh screen and then removing the smaller particles by washing with acetone. This proved to be very satisfactory in that the flow of the particles in the feeder was better than those prepared by the first two methods.

Source material requiring additional amounts of doping material were prepared by evaporating the dopant onto wafers of GaAs in a vacuum of about 10^{-4} Torr. The wafers were cleaned in an ultrasonic acetone bath immediately before placement in the vacuum chamber. The amount of additional doping material was determined by the weighing of the wafers before and after evaporation. The wafers were then crushed as described above.

The Evaporation Procedure

Although the substrate temperature, the source temperature, the source-to-substrate distance and the rate of deposition were varied from experiment to

experiment, the pumpdown procedure remained the same. Figure 16 shows the experimental setup using the disc substrate heater and the horizontal source. The setup remained essentially the same for different substrate and source heaters.

The system was initially pumped down to about 10^{-5} Torr at which time all heating elements were turned on to outgas the system. This outgassing process varied from 15 to 30 minutes. After a cooling down period of at least three hours, nitrogen was introduced into the system to raise the pressure to about 0.015 to 0.02 Torr. The substrate was then cleaned by ion bombardment.

After the ion bombardment step, the system was again pumped down to about 10^{-5} Torr where the system was outgassed again by turning on all heating elements. A third outgassing was done when the system attained a pressure of about 10^{-7} Torr. The three outgassing steps minimized the problem of excess residual pressure, as the system normally remained at pressures below 10^{-6} Torr for up to one hour with all heaters on during the evaporation process.

After the deposition step, the system was kept at the final deposition pressure or lower for a cooling period of at least two hours. Following the cooling period, nitrogen was introduced into the system to bring it up to atmospheric pressure.

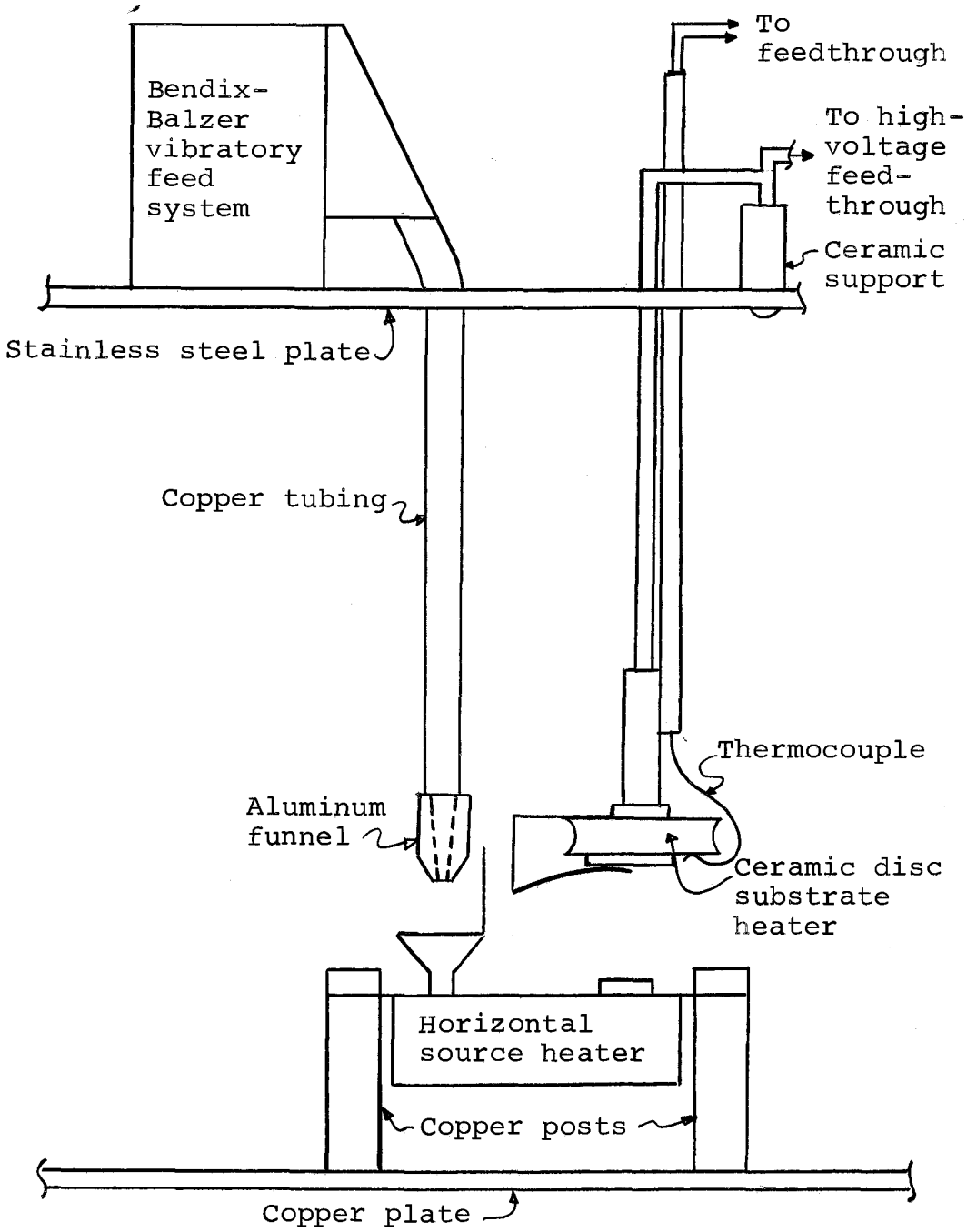

Figure 16. Experimental setup using the ceramic disc substrate heater and the horizontal source heater.

IV. EXPERIMENTAL RESULTS

The substrate temperature, the type of substrate and the type of evaporant material were found to be the major factors which determined film properties. The range of substrate temperatures used varied from the ambient to 650°C. The ambient temperature depended on the source heater used and the source-to-substrate distance and ranged from about 50°C to 350°C. The different substrates used included etched GaAs, mechanically polished GaAs, germanium, sapphire and glass.

Two types of evaporant material were used. These were the normally available GaAs with resistivities varying from 0.01 ohm-cm to 6×10^{-3} ohm-cm and specially prepared GaAs in which an additional amount of doping material was included.

This chapter first considers the structural and optical properties of the films and then presents the electrical properties of these films.

Crystallinity of Evaporated Films

The crystal structures were studied using a Norelco x-ray diffractometer made by North American-Phillips using a Cu target and a Ni filter. For films deposited on glass substrates, substrate temperatures in the 150°C to 250°C temperature range yielded films that were

amorphous. Polycrystalline films were grown at higher temperatures but no single crystal films were found. The diffraction peak occurred at a 2 Θ angle of 27.3° which is indicative of the (111) plane in GaAs.

Films grown on single-crystal GaAs and single-crystal germanium also showed peaks at 2 Θ values of 27.3°. Whether these films were single-crystalline or not could not be determined by the available equipment. However, Müller (40) has shown by extensive electron diffraction and x-ray studies that deposition on single crystal substrates tended to yield single crystal films for III-V semiconductors at elevated temperatures. Müller further points out that structural defects do exist and are due to stacking faults of the (111) planes, and also that although the (111) structure is well formed, growth takes place without generally being parallel to the substrate or perpendicular to the vapor beam. These defects were not studied in this experiment due to lack of equipment, but from the electrical data, it is reasonable to assume their existence.

To check stoichiometry, GaO and AsO_2 were mixed in a mole ratio. The fluorescence after x-ray bombardment was noted and this was compared with the fluorescence of the deposited films. Figure 17 shows the plot of intensity versus the 2 Θ angle for the molar standard

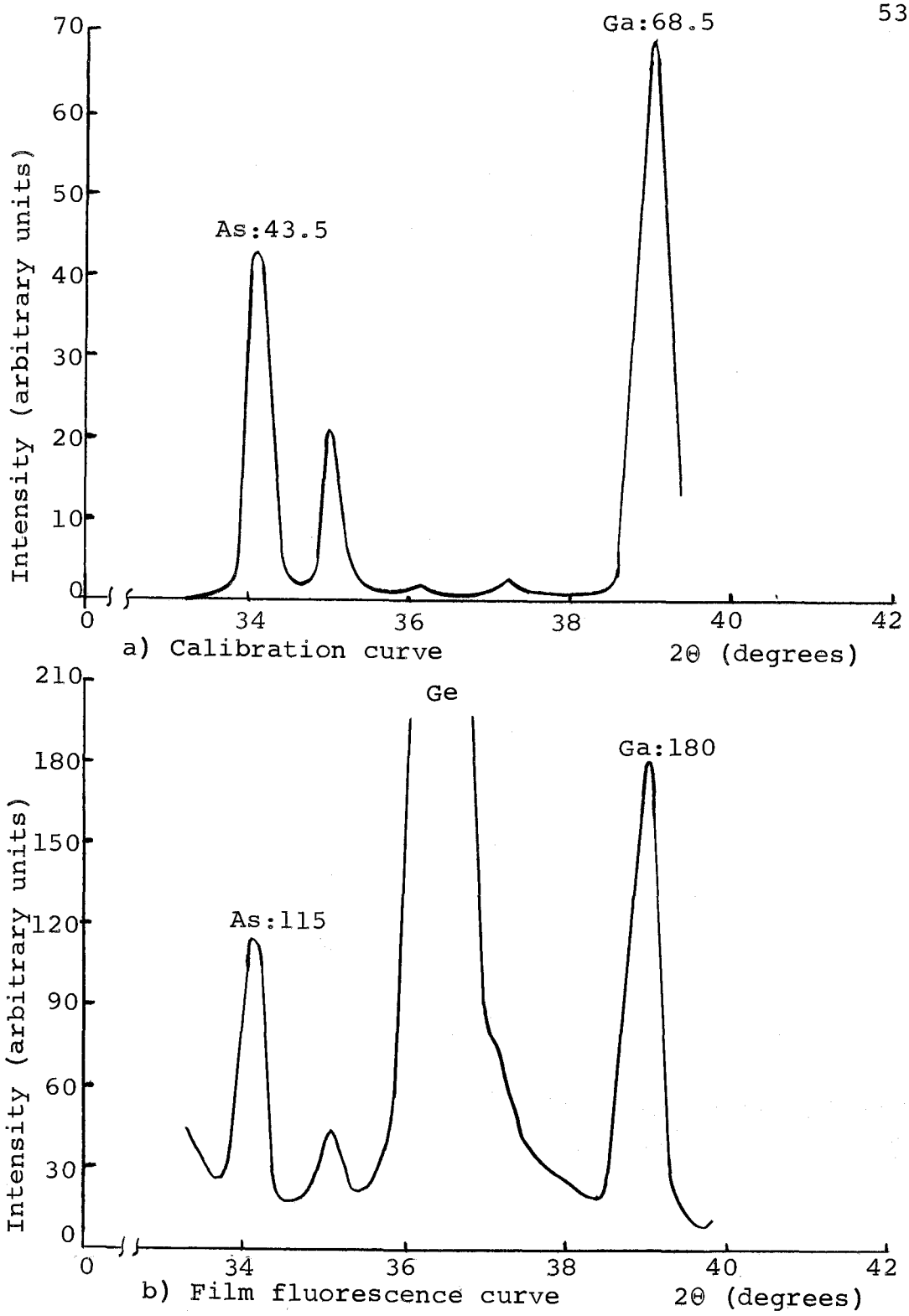

Figure 17. Fluorescence curves used to determine film stoichiometry.

(curve a) and for a film grown on a germanium substrate (curve b). The intensity ratio for the standard is 68.5/43.5 or 1.57. For the evaporated film the ratio is 180/115 or 1.56 which indicates that the films are stoichiometric.

Optical Measurements

Several of the low-resistivity films and some zn-doped films were studied by optical methods. Figure 18 shows the results as obtained on a Perkins-Elmer Model 450 UV-Visible-NIR Spectrometer.

The output of the spectrometer is given in absorbence. To convert this data to absorption coefficient, the following relation was used:

$$A = \alpha bc$$

where A is absorbence, α is the absorption coefficient, b is the sample thickness and c is the concentration which is equal to one for this case.

Taking the definition of band gap as that energy where the absorption coefficient is one-half the maximum value, values for e_g for the evaporated films ranged from 1.47 ev to 1.80 ev. The value for bulk GaAs given by Sturge for this type of measurement is 1.43 ev.

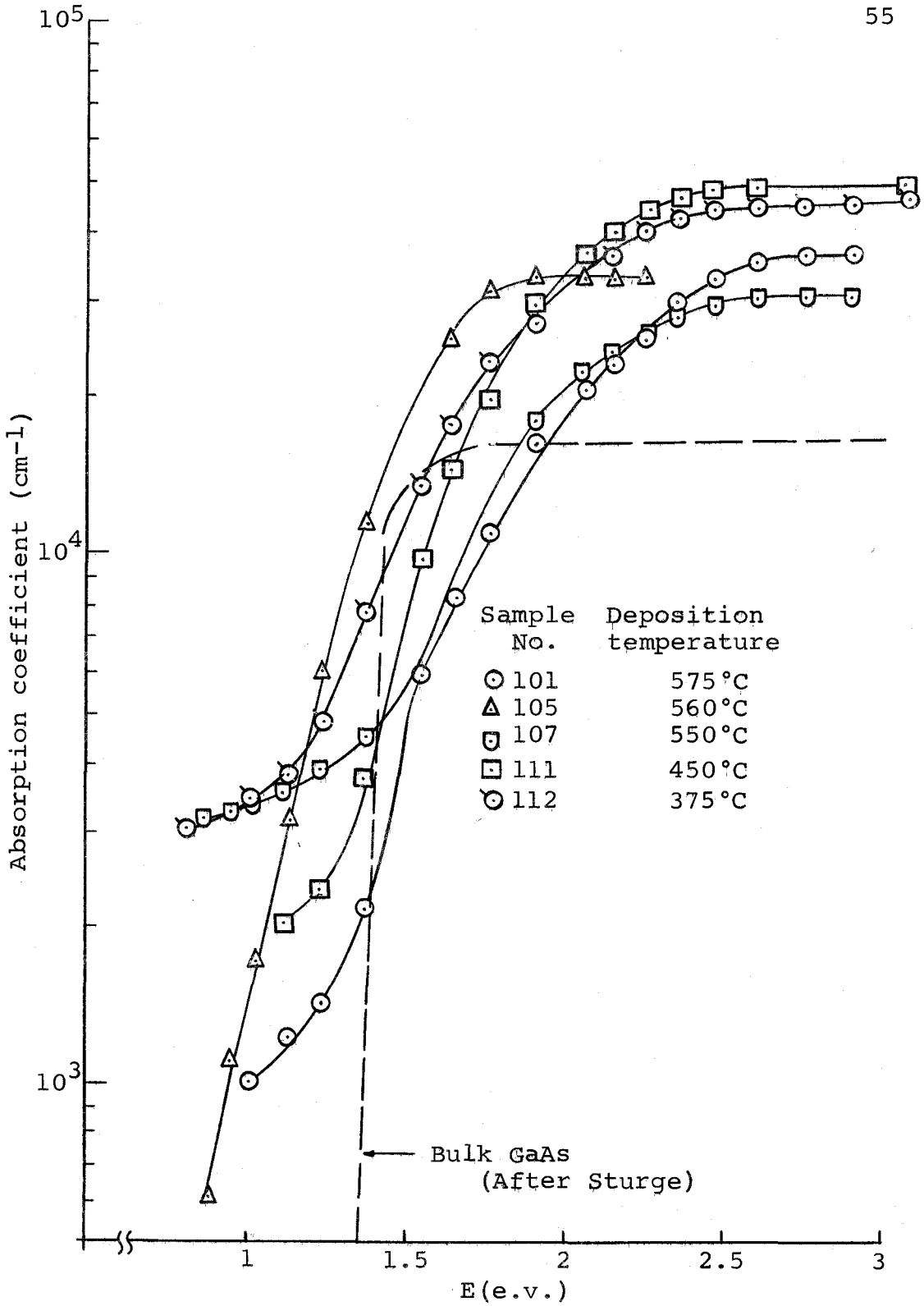

Figure 18. Optical absorption coefficient versus energy of incident light for low-resistivity films.

High-Resistivity Films

In the initial phase of the experiment, the resultant films had very high resistivity. Crushed material varying in initial resistivities from 0.01 ohm-cm to 6×10^{-3} ohm-cm and of both the n- and p-types were used. Substrate temperatures ranged from ambient to 650°C. Source-to-substrate distance was varied from one inch to ten inches and the source temperature was in the 1350°C to 1800°C range. Deposition rates were determined to be from 2Å/second to 600Å/second.

Films grown on insulating substrates such as glass, ceramics and sapphire showed less than one microampere at 200 volts. Films on conducting substrates exhibited V-I characteristics as shown in Figure 19. The three different curves are the result of three different placements of the probe. Curve A is that seen with both probes on the film, curve B is that seen with one probe on the film and the other on the substrate, and curve C is that with both on the substrate.

The "breakdown" voltage of curve B is of particular interest. If a true semiconducting film were present, curve B should be similar to curve A in one direction and to curve C in the other. The symmetric nature of the and the breakdown of B being about one-half that of C is typical of what would be observed on thin insulating

films.

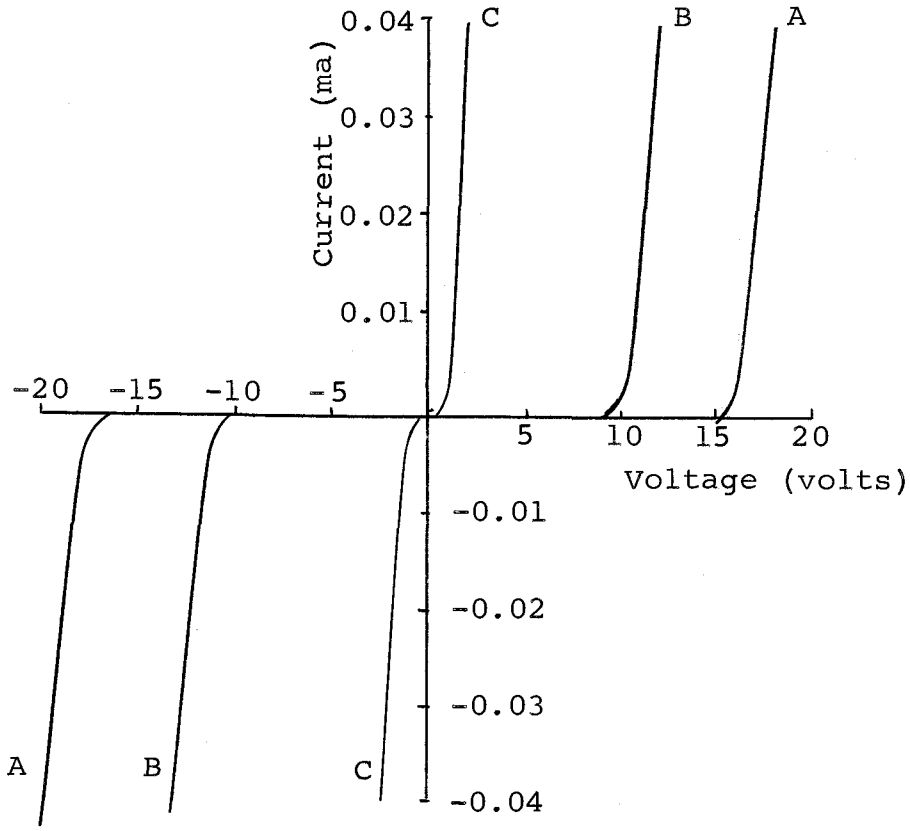

Figure 19. V-I characteristics of high-resistivity GaAs films grown on a germanium substrate.

Although most films exhibited the 2 to 1 difference in breakdown voltage between curves A and B, film thickness did not determine the breakdown voltage. In fact, no correlation between the breakdown voltage and any of the growth parameters could be found. Table I lists a sampling of films listing their film-film breakdown voltage and their growth conditions. Over 80 films were grown under differing conditions with the resulting voltage-current relation similar to the curves shown in

TABLE I. Growth Conditions and Breakdown Voltage for Some High-Resistivity Epitaxial GaAs Films.

No.	Breakdown Voltage (volts)	Substrate	Thickness (μ)	Rate of Growth (A/sec)	Substrate Temp. (°C)	Source Temp. (°C)
A6	25	GaAs	0.9	5	590	1590
A7	14	GaAs	1.8	5	500	1530
C7	46	Ge	0.6	7	535	1580
D1	44	GaAs	0.6	5	500	1550
D2	35	Ge	1.7	19	525	1550
D3	35	Ge	1.8	20	525	1550
F3	35	GaAs	1.5	25	300	1350
F4	64	GaAs	1.5	50	500	1500
F5	70	GaAs	1.5	25	525	1500
H1	17	GaAs	0.3	6	525	1500
H2	16	GaAs	0.3	5	310	1510
H7	35	GaAs	0.5	16	525	1410
I1	90	GaAs	0.7	14	550	1400
I2	100	GaAs	1.2	40	500	1300

Figure 19.

The effects of annealing were studied. Samples were sealed in a quartz ampoule at pressures less than five microns. About 20 mg of GaAs powder was included in the ampoule to provide additional arsenic pressure. At low annealing temperatures (less than 400°C) no change was noted even at annealing times of 72 hours. For 90 minutes of annealing at 700°C a shift to lower film-film breakdown voltage was noted. However, for longer annealing times the V-I characteristics tended to become ohmic.

Samples were also annealed in vacuums of less than 10^{-3} Torr. No change was noted in films annealed for one hour to 72 hours for annealing temperatures up to 450°C. For temperatures of 525°C and higher, long annealing times tended to evaporate the films. The resultant surfaces were silvery and rough and made ohmic contacts to tungsten point probes. This would suggest that the annealing process at elevated temperatures in vacuum removed the arsenic atoms from the films, leaving gallium on the substrate.

Low-Resistivity Films

To increase the conductivity of the evaporated films, excess doping material was incorporated in the evaporant powder. This was accomplished by vacuum depositing tin (or zinc) on an n- (or p-) type GaAs wafer before crushing. A range of 0.5 to 6% for tin and 1% to 9% for zinc was studied.

The pressure during deposition was kept at below 10^{-3} microns. The horizontal source heater was used at a temperature of 1350°C and the source-to-substrate distance was two inches. Rates of deposition varied between 50 and 65 Å per second.

Figure 20 shows the variation of resistivity to percent tin for the cases where the substrate temperature was held at about 570°C. As expected, the resistivity decreased as more tin was added.

Using a 3.2% tin source, the substrate temperature was varied between 200°C and 600°C. The horizontal source was used and the source-to-substrate distance was two inches. The pressure was kept below 10^{-3} microns. Figure 21 shows the variation of resistivity versus substrate temperature.

Films deposited below 300°C substrate temperature showed conduction of less than one microampere at 200 volts. One attempt was made at a substrate temperature

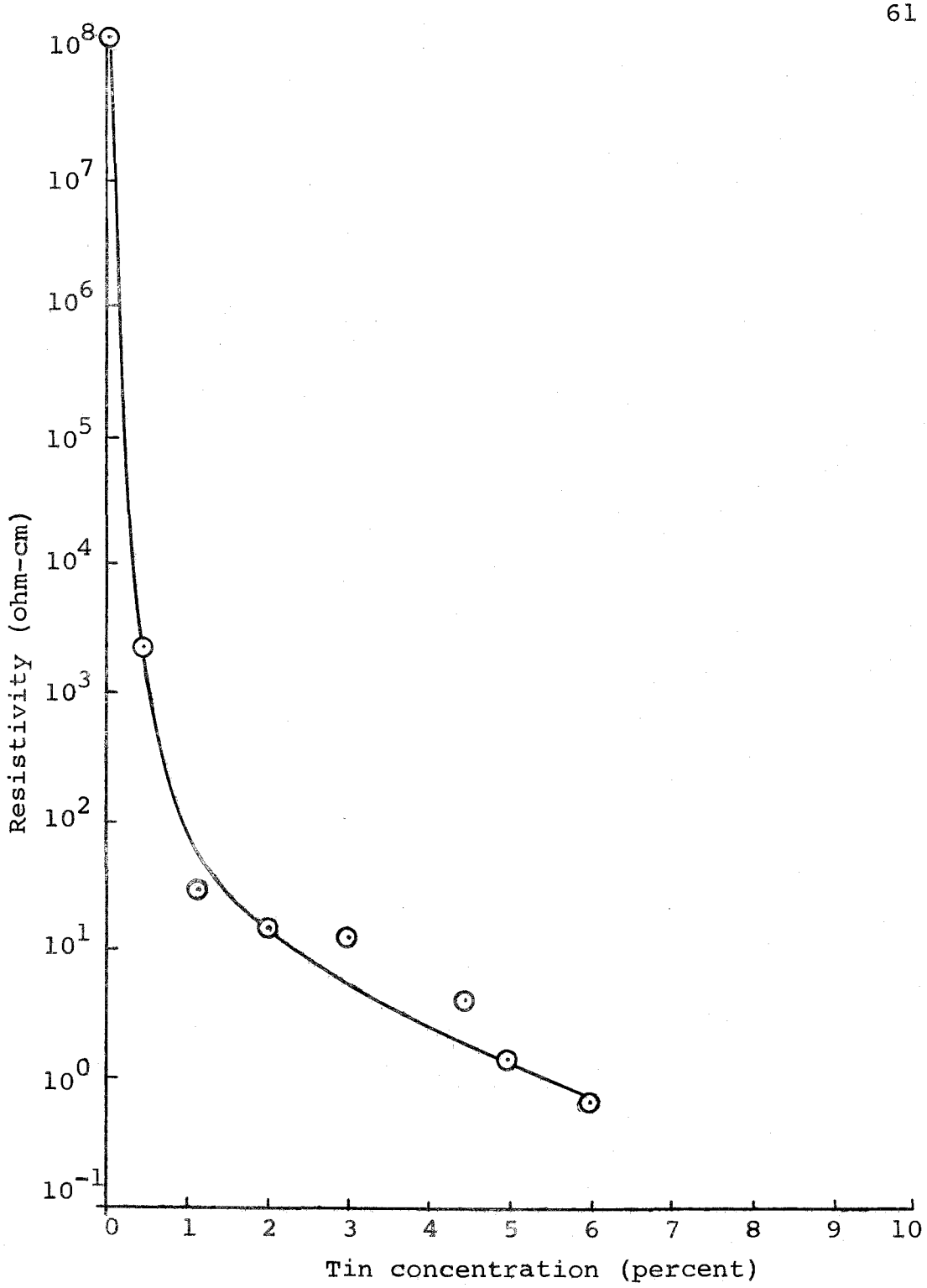

Figure 20. Resistivity versus percent tin for GaAs films grown at a substrate temperature of 570°C.

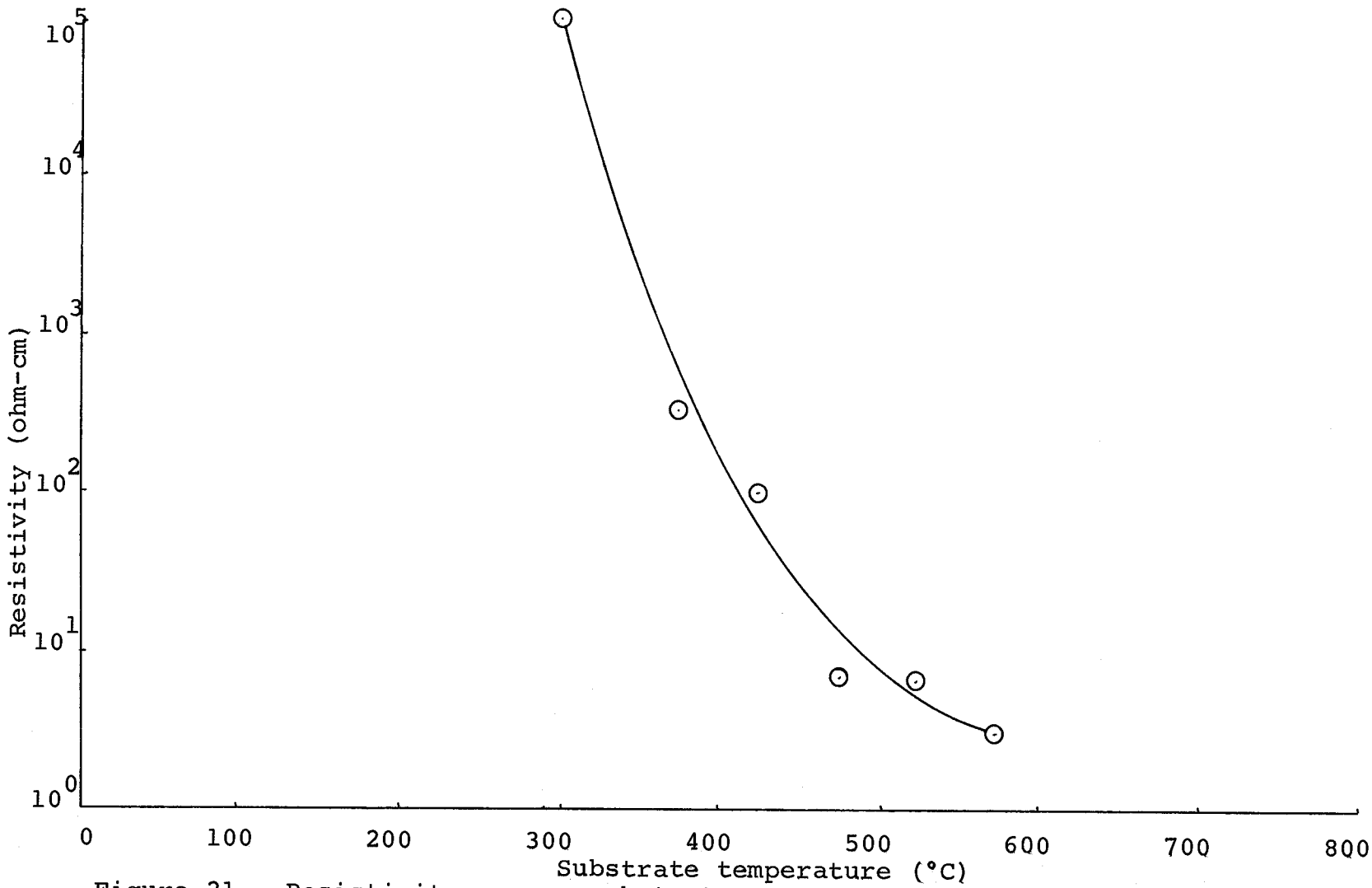

Figure 21. Resistivity versus substrate temperature for GaAs films with 3.2% tin in the evaporant material.

of 675°C. The resulting film proved to be gallium for the most part, and film thickness was less although the feed rate was increased and the time remained constant. This was expected, as Müller (41) and others have noted a critical temperature in this range. At this temperature the forming crystal is unable to hold the arsenic atoms in the crystal structure because of the resulting arsenic vapor pressure.

Various concentrations of zinc from 0.5% to 9% were tried but no conduction was noted in these films. At 200 volts the current was less than one microampere.

A thermoelectric p-n indicator showed a definite n-type deflection for the lower resistivity (tin) films. The higher resistivity films including the zinc films did not show any noticeable deflection.

For these low-resistivity films, the change in resistivity with respect to temperature was studied. At sufficiently high temperatures all films exhibited a slope approximately equal to the theoretical intrinsic value. Also, all films showed a negative temperature coefficient of resistance as expected for semiconductors. Figure 22 shows the experimental results and includes an intrinsic line as determined by Folberth and Weiss (16).

An expanded graph of the intrinsic region of Figure 22 is shown in Figure 23. The band gap in the intrinsic

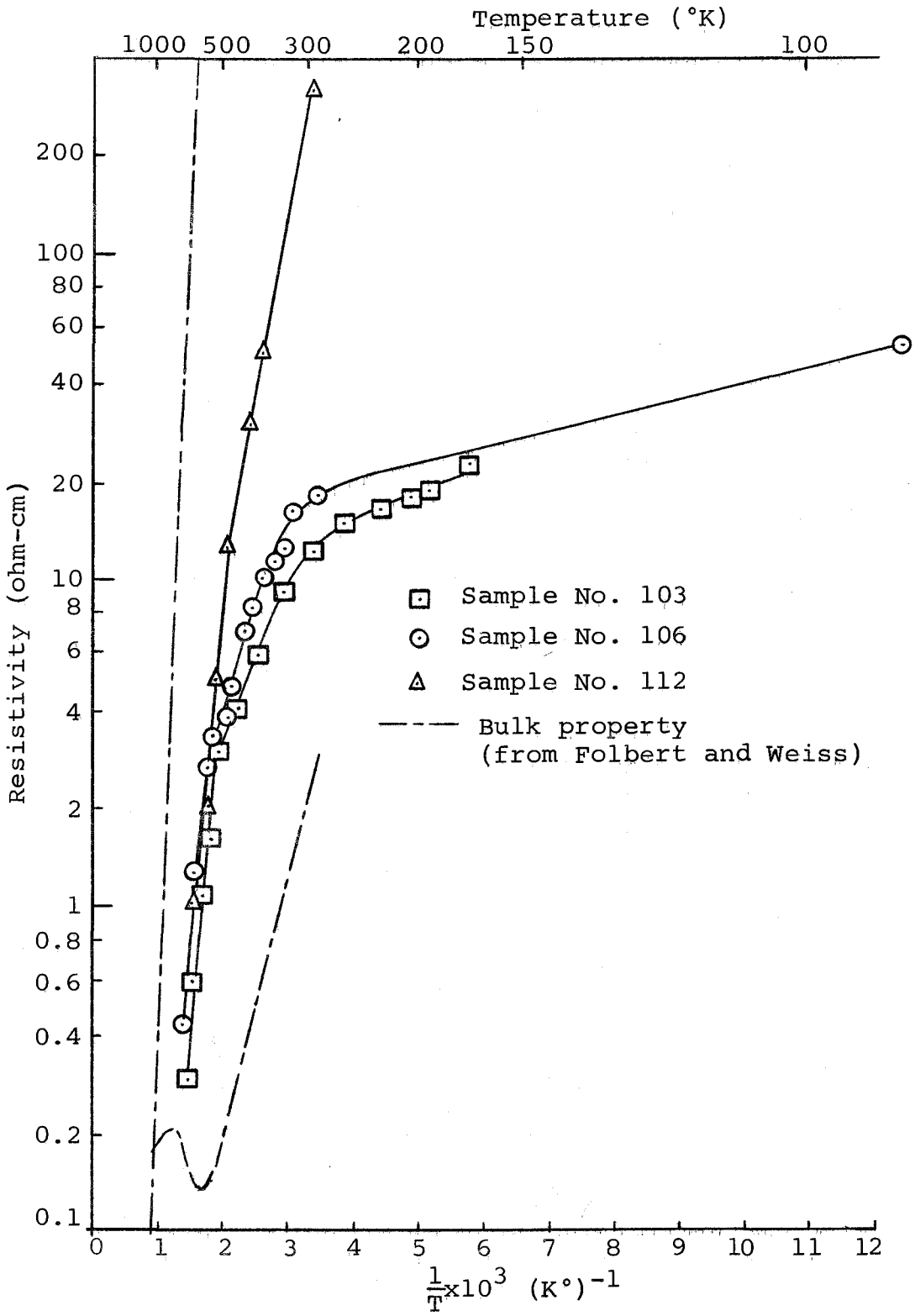

Figure 22. Temperature dependence of low-resistivity flash-evaporated GaAs films grown on sapphire substrates.

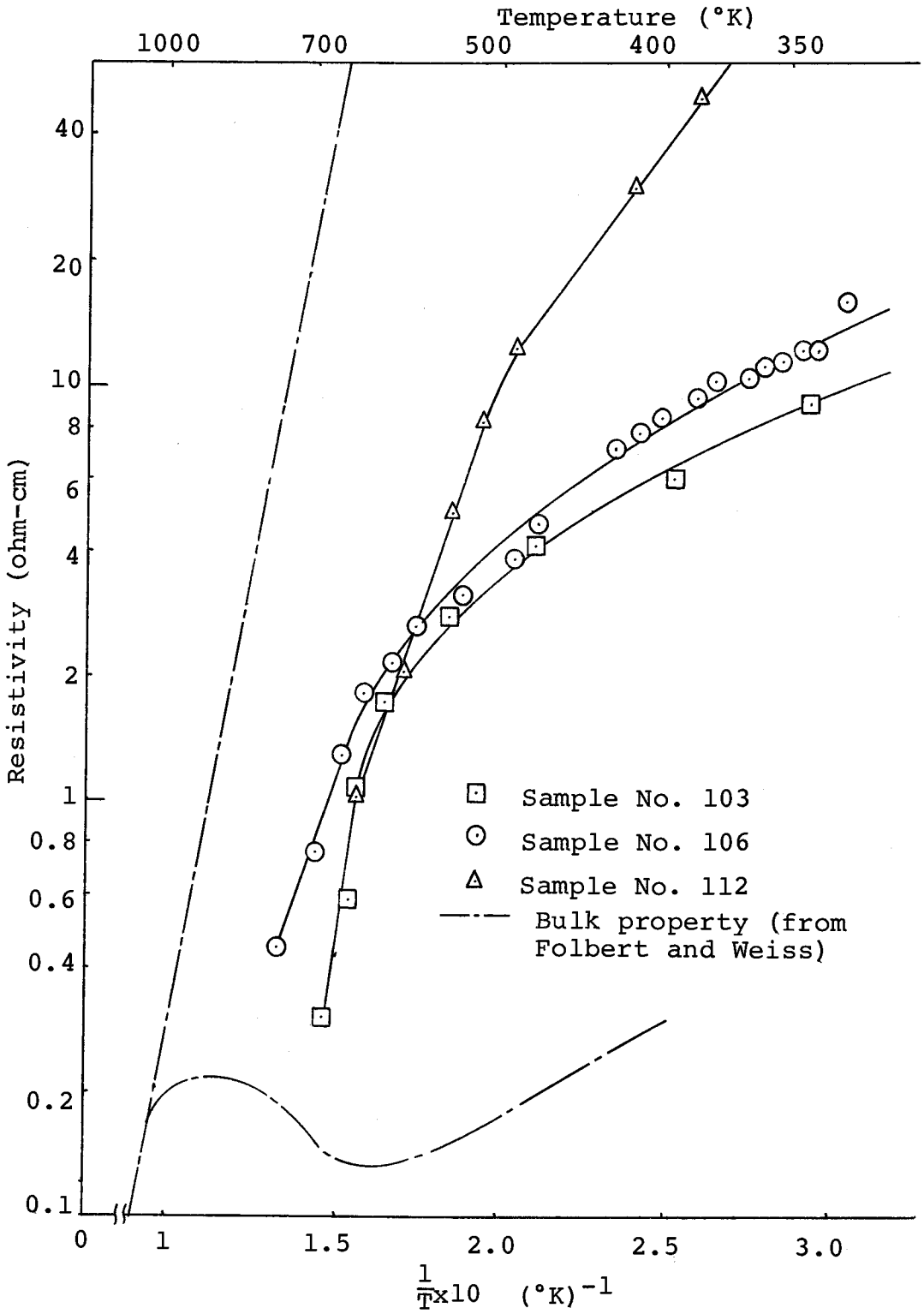

Figure 23. Expanded graph of the intrinsic portion of the curves shown in Figure 22.

region can be calculated from the relation

$$e_g = 2k \frac{\Delta \ln \rho}{\Delta \frac{1}{T}} \quad \text{where } k = \text{Boltzman constant}$$

$$= 0.86 \times 10^{-4} \frac{ev}{°K}$$

$$= 0.172 \times 10^{-3} \frac{\Delta \ln \rho}{\Delta \frac{1}{T}} \text{ ev.}$$

Since the intrinsic region occurs at high temperatures, only an approximate value of band gap can be calculated by this method. The values obtained for band gap energy varied between 1.18 to 1.72 ev. These values are comparable to the experimental values of about 1.4 ev given by Folberth and Weiss for bulk GaAs.

Hall Effect

Hall effect measurements were made on various films. The samples were cut using positive photo-resist techniques and etching with 1:1:2 HNO_3:HCl:H_2O. They were then mounted on a fiber-glass holder with wax and conductive paint was used to make electrical contact. A 3650 gauss permanent magnet was used as the magnetic field source.

In most samples, voltages that could unambiguously be attributed to the Hall Effect were not observed. The largest Hall voltage measured was for a film grown at 575°C with 4.5% tin added to the evaporant material. The polarity indicated n-type conduction and the magnitude of the voltage was two millivolts for three

milliamperes of current.

Diode Action

Tin-rich GaAs powder was evaporated on p-type GaAs and sapphire substrates. The source temperature was 1350°C, the substrate temperature 525°C to 575°C and the source-to-substrate distance was two inches. The rates of deposition varied from 12 Å/sec to 56 Å/sec and the pressure in the evaporation chamber was always below 10^{-6} Torr during evaporation.

For the films grown on sapphire substrates both zinc and tin made ohmic contacts to the films. Normally, since zinc is an acceptor impurity in GaAs, a rectifying contact would be expected. Alloying the zinc for different lengths of time resulted in no appreciable change.

A tungsten point made a rectifying contact with the films, however. Figure 24 shows the V-I characteristics for a case where one probe was placed on a tin dot and the other on the bare substrate. This film was deposited at 575°C at a deposition rate of 56 Å per second. The evaporant contained 4.5% tin by weight. With both probes on tin dots, the V-I curves were linear and the resistance value was noted as 2600 ohms.

Some evaporant with 4.5% tin by weight was evaporated on a p-type GaAs substrate. The substrate

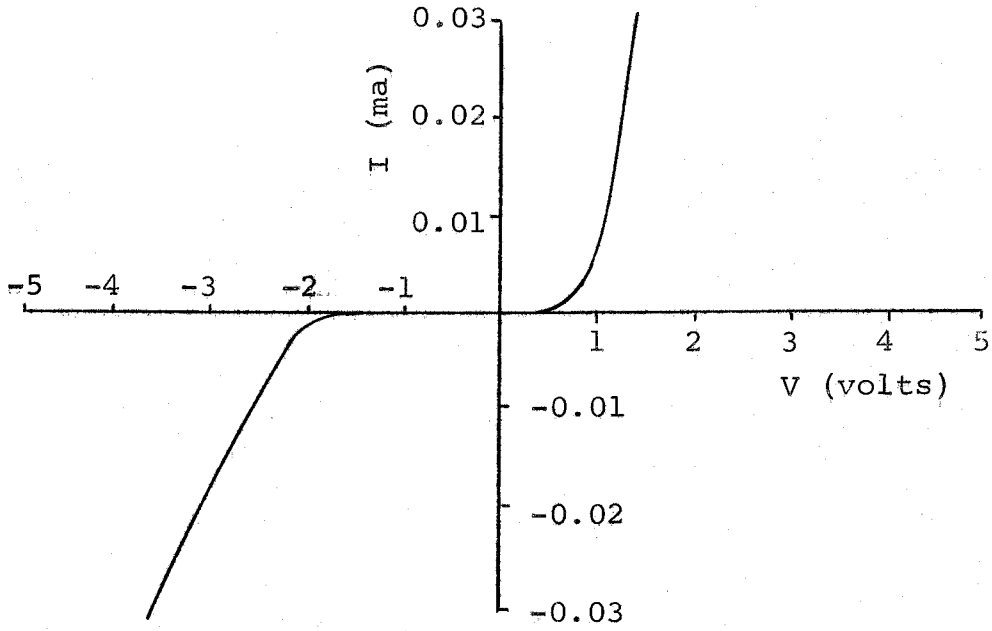

Figure 24. V-I characteristics for a point-contact diode on a film deposited from GaAs powder containing 4.5% tin.

temperature was 550°C and the deposition rate was 55 Å/sec. The substrate was about 0.015 ohm-cm and cadmium doped. Figure 25 shows the resulting V-I characteristics.

The contacts were made by thermocompression techniques using the Kulicke and Soffa Model 401U wedge bonder. One mil gold wire was used as the lead material. The substrate was attached to the header using a Au-Si alloy.

Three contacts were made, one from the topside of the substrate and two from the film surface. The V-I

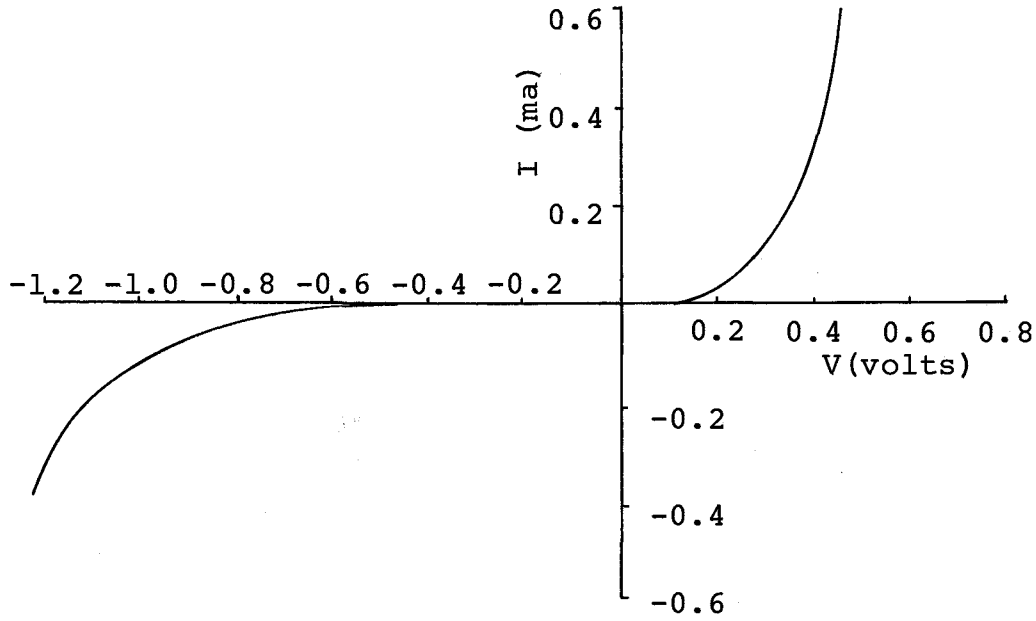

Figure 25. V-I characteristics of a diode grown by evaporating 4.5% tin-doped GaAs on a p-type GaAs substrate.

curve between the two leads from the film surface was ohmic and had a value of 44 ohms. That between the top-side lead from the substrate and the bottom of the substrate was slightly nonlinear and had approximately 80 ohms contact resistance. Since these are practically shorts compared to the reverse characteristics, the diode effect can confidently be assumed as a property of the film-substrate interface.

Several diodes were fabricated using the film discussed above. The characteristics were similar in all cases. Others were fabricated using films with 3.2% and 4% tin and similar V-I curves were observed.

Light Emission in GaP Semi-Insulating Films

Light emission was noted in gallium phosphide films evaporated on gallium arsenide substrates at various substrate temperatures. The films were prepared using the horizontal source at a temperature of 1350°C. The source-to-substrate distance was 1.5 inches and the system was held at below 10^{-3} microns. Film thickness was about one micron and the rate of deposition was 20-30 Å per second. The resulting films were of very high resistivity.

Thin films of zinc and tin were deposited on the film in the circular areas of 10 mils and 25 mils diameter. The metallic films were about 1000 Å thick. Light emission was noted around the edges of the metallic contacts.

To increase the total light emitted, Ag was evaporated in 25 mil diameter circular areas 50 Å thick. 50 Å of Ag allows an optical transmission of about 50%. Light emission was observed through the entire Ag film.

The spectrum of the emitted light was observed using a Jarrell-Ash 0.25 meter Ebert monochrometer and photo-multiplier tube. The block diagram of the measuring apparatus is shown in Figure 26. The output spectrum is shown in Figure 27 along with the spectrum obtained for a tungsten filament at 1670°C. The similarity

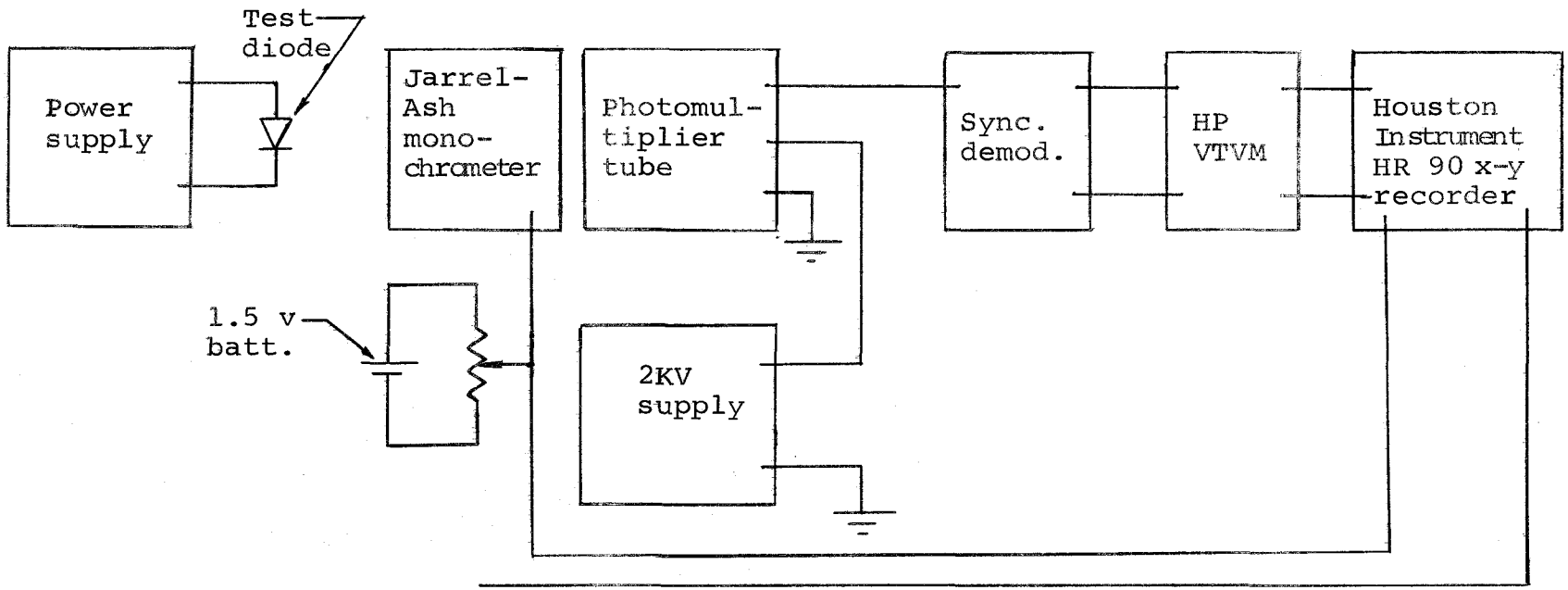

Figure 26. Block diagram of the apparatus used to measure the light emission spectrum from high-resistivity GaP films.

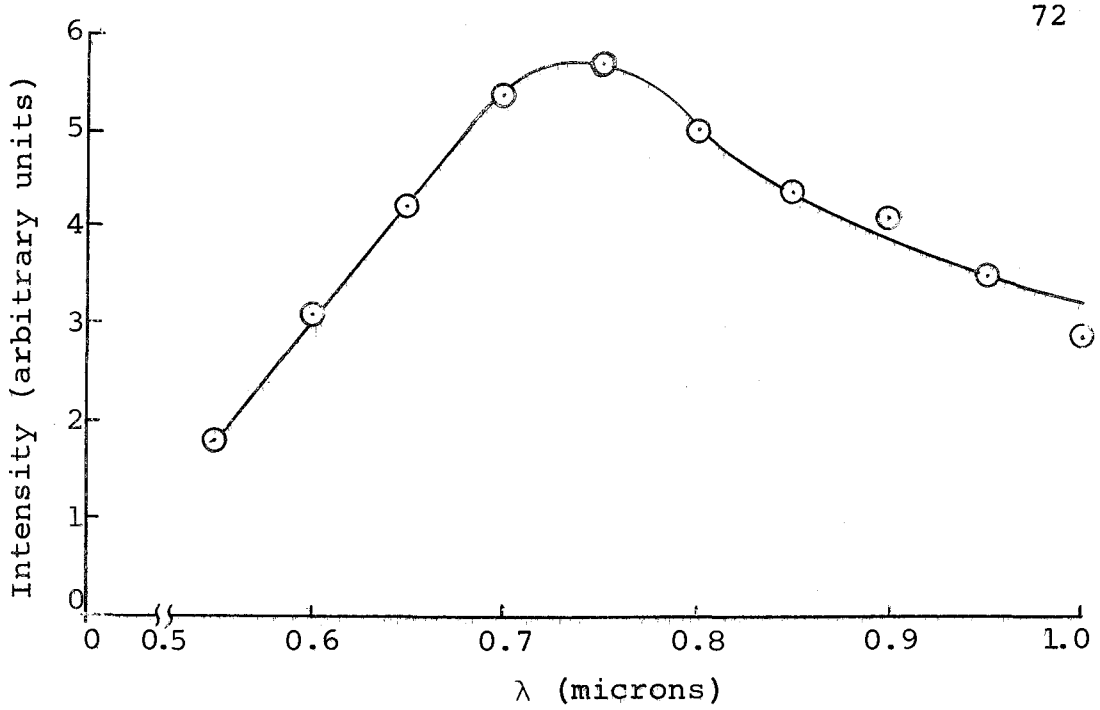

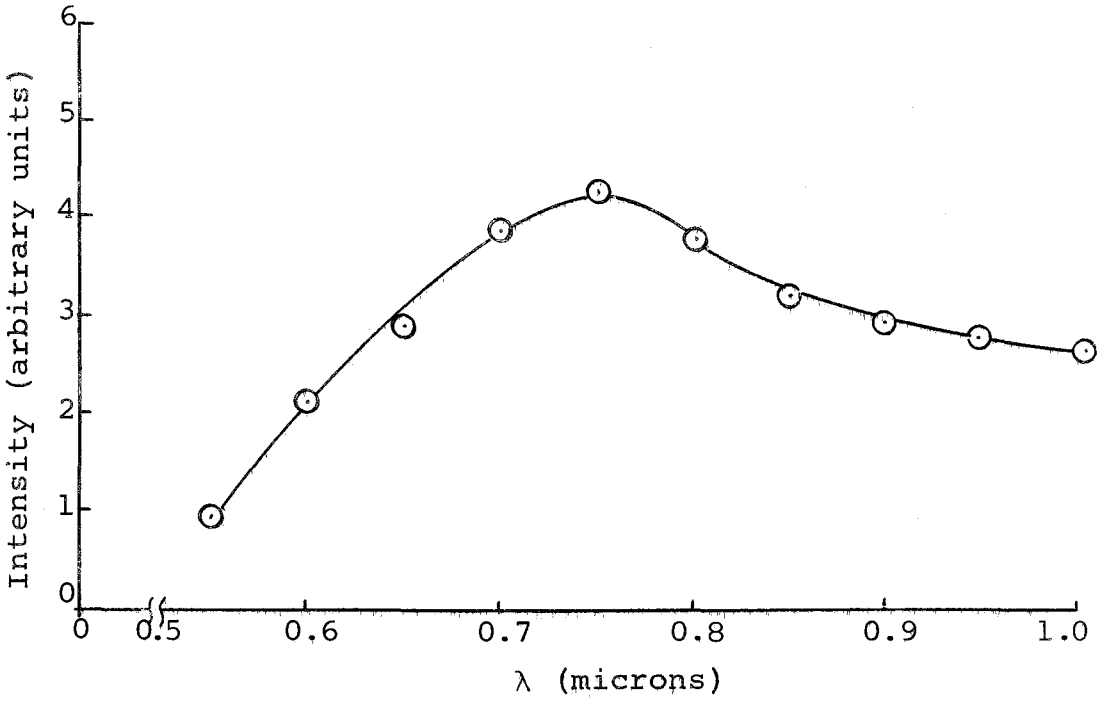

Figure 27. Spectral response curves for a Tungsten filament at 1670°C (upper curve) and a high-resistivity GaP film (lower curve).

indicates that these GaP diodes emit "white" light.

The intensity of emitted light increased with increasing current. Initial emission occurred in spots across the metallized areas and more spots were seen as the current was increased. A typical V-I curve is shown in Figure 28.

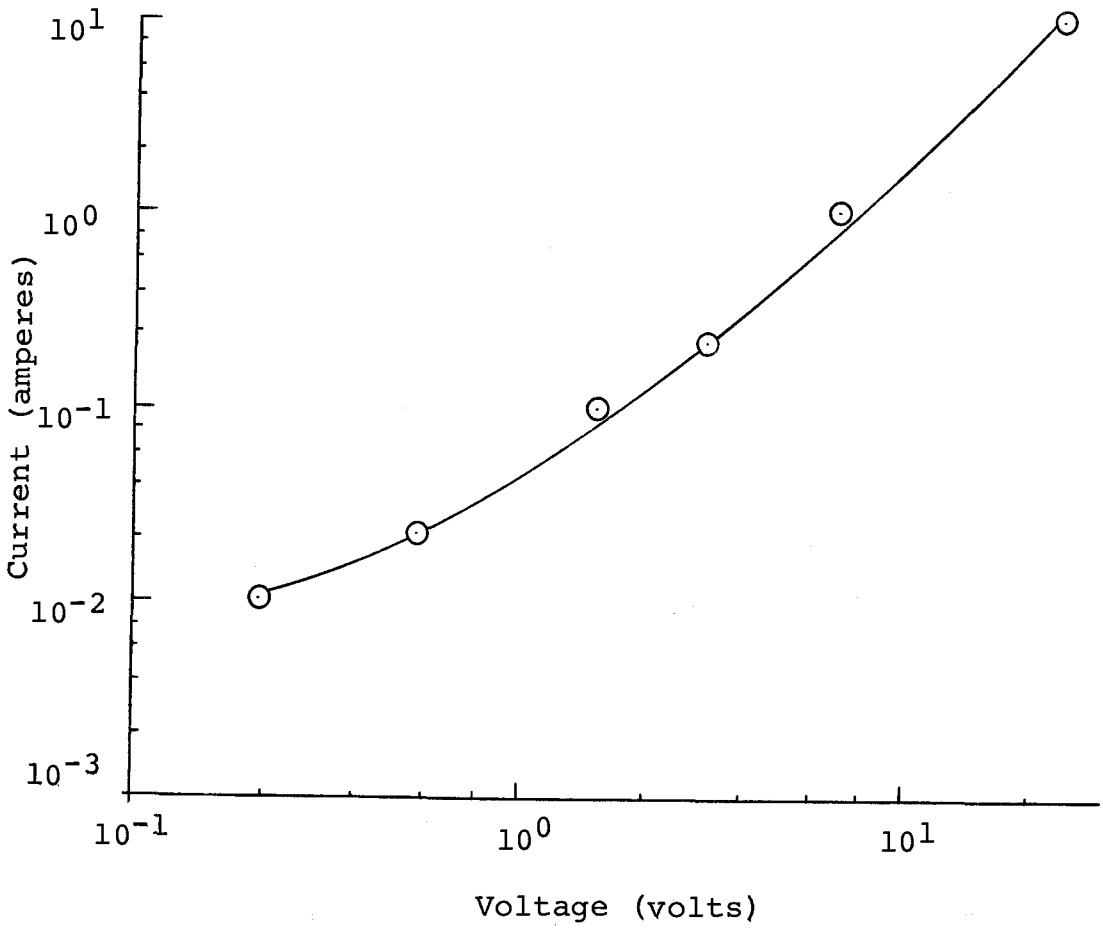

Figure 28. Typical V-I curve for the electroluminescent devices studied.

With contacts made to two metallized dots, the emission could be shifted from one dot to the other depending on the polarity of the applied voltage. Emission occurred on the dot which had the metal negative with respect to the semiconductor. For the opposite polarity an orange emission was observed. This emission disappeared permanently, however, when a certain level of current was applied. The exact current level was difficult to pinpoint but was around 15 ma for the 25 mil dots.

To determine where the light emission was taking place, a wafer was cleaved across one of the Ag dots. Current was applied and the emission center was noted as being below the film surface and approximately at the film-substrate interface. The emission was not uniform across the junction but tended to occur in spots. The number of light emitting spots increased with increasing current. These conditions are similar to what Gershenzon and Mikulyak observed in zinc-diffused GaP diodes.

V. DISCUSSION OF RESULTS AND SUMMARY

In this chapter, correlation between the experimental and theoretical results is presented and the results are summarized. The observation of the structural properties in the results section is in agreement with previous work on germanium, silicon and III-V compounds. That is, the significant parameter is the substrate temperature. At low temperatures the films grown are amorphous while at higher temperatures films become crystalline.

In the next section the results of the optical observations are discussed. Then, a discussion of the electrical properties is presented, followed by a section on the observations of electroluminescence in the films. The final section summarizes the important points of this project.

Optical Properties

The curves shown in Figure 18 are similar to those obtained by Davey and Pankey (11) for their films grown by the three-temperature method. A downward energy shift with decreasing substrate temperature was not noted in this experiment. This is not in conflict with the results of Davey and Pankey, however, since their substrate temperatures were below 400°C.

An alternate definition for band gap may be taken as done by Davey and Pankey. Taking the arbitrary absorption coefficient value of 10^4 cm^{-1} as the band energy determining point, the range of band energies is then 1.34 ev to 1.72 ev. This agrees more closely with those obtained from the resistivity data.

Comparison of the experimental curves with the bulk curve done by Sturge shows a considerable broadening in the experimental curves. This can be explained following the method of Glass (20). If a specimen has internal strains, E(xyz), then the absorption coefficient is not uniform but dependent on the strain density. The effect of E(xyz) is to shift the band edges through energies given by

$$\Delta E_{\pm} = a'\sum_i \epsilon_{ii}(xyz) \pm \frac{1}{2}\left[b^2\sum_{i,j}(\epsilon_{ii}\ \epsilon_{jj})^2 + 2c^2\sum_{i,j}\epsilon_{ij}^2\right]^{\frac{1}{2}} .$$

a' is the pressure coefficient of the band gap and b and c are the [100] and [111] shear deformation potentials. As can be seen, the strains determine $\Delta E_{\pm}$ which in turn determines the band gap for a particular area of the specimen. This means that if the strains are not identical over the volume of the specimen, the band gap also varies throughout the volume. The result is that only the portions of the crystal with the band gap less than the energy of the impinging light rays absorb energy,

and the total absorption coefficient is really an average of a number of different coefficients corresponding to the various individual areas. This averaging results in the broadening of the absorption curve.

Since the band gap from the optical data is defined as the energy value at half the maximum absorption value, $\Delta E_{\pm}$ has a significant effect on the value of E_g. In some cases it may be possible that the strains affect the absorption curve in a symmetric manner about E_g, but in most instances, this is probably not the case. This results in the value of E_g being shifted above or below the value that a strain-free observation would yield.

High-Resistivity Films

There are several models that can be presented to explain the reason for the high resistivity values of the films obtained in the initial phase of the experiment. The use of the "60 dislocation" is a highly plausible model since this type of dislocation is known to be important in III-V compounds. It is shown in Figure 29. Only three atoms surround each of the identical atoms located along the dislocations. Whether these sites have a donor or acceptor nature depends on the type of atom located at the dislocation. If the atom is trivalent no excess valence atoms exist. Hence, the

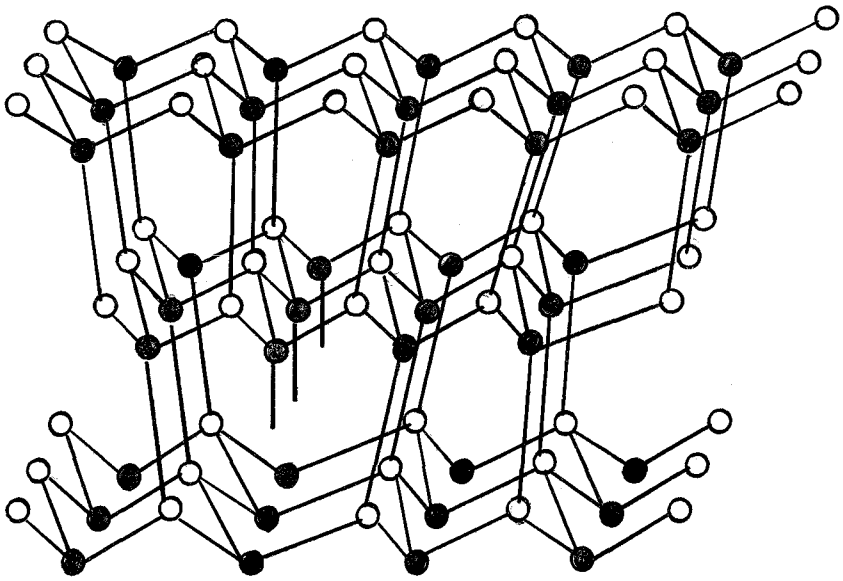

Figure 29. Zinc-blende lattice showing a 60° dislocation. (From Madelung).

dislocation is like an acceptor in nature. If the atom is pentavalent, each atom has a filled electron pair and is donor in nature. This is in contrast to silicon and germanium where the dislocation is an acceptor after losing the extra valence electron or donor upon taking an extra electron and forming a saturated pair.

Another model involves the deep levels introduced by impurities. For instance, oxygen and copper are known to introduce deep states. They are also multi-level and therefore the amount of impurity introduced is not critical. If copper or oxygen were the impurities introduced, the resulting film should be high-resistivity n-type material, according to Madelung (38). In the

experiment, p-type high-resistivity films were found in many instances and so this mechanism probably is not the cause for the high-resistivity films.

A third model suggests that in the evaporation process, the impurity atoms of the source material are not incorporated in the growing film. In silicon growth by pyrolytic methods this has been found to be the case in some instances. The impurities may have not been evaporated in the first place, or upon reaching the substrate a segregation effect may have taken place as happens in zone-refining processes.

Low-Resistivity Films

With the incorporation of additional tin in the source material, relatively low-resistivity n-type films were grown. Resistivities as low as 0.6 ohm-cm were obtained as compared to the greater than 10^8 ohm-cm measured for films without additional tin provided.

One possible explanation for the lowering of resistivity values is to consider a model in which the additional dopant provides more carriers than there are traps. Then, the carriers not held in trapping levels will be free for conductive purposes. While this model explains the lowering of resistivities of tin-rich films, it does not readily explain the reason for the

high-resistivity of zinc-rich films.

An alternate model concerns the fact that in diffusion processes, dopant material tends to collect at dislocations. Since the crystallite interfaces are the regions of highest resistance in a polycrystalline material, the congregation of tin atoms at the interfaces would tend to lower the resistivity of the crystal by providing an electrical bridge between crystallites. The reason for the high resistivity for zinc-rich films is again not obvious. The answer may lie in the ease of conduction at a tin-GaAs interface as compared to a zinc-GaAs junction.

Unlike the results of Davey and Pankey who found that the minimum of the resistivity-versus-substrate temperature curve occurred at a substrate temperature of 280°C, no such minimum was found in this investigation. As Figure 21 shows, resistivity is a decreasing function of substrate temperature. Since Davey and Pankey used the three-temperature technique, however, the discrepancy may not be significant even though both processes involve vacuum deposition.

Hall Effect

The measured Hall voltages were far below what was theoretically expected for GaAs films. The largest Hall

voltage measured was 2 mv. The Hall mobility derived from this value is about 0.7 cm^2/v-sec. This is much less than that measured for bulk material where the highest reported value is 8500 cm^2/v-sec (38).

Since vapor deposited epitaxial films are known to contain large numbers of dislocations, it is reasonable to assume that the low mobility values are the result of scattering by the dislocations. Also, the films from which the Hall samples were cut were polycrystalline and this tends to reduce the mobility of free carriers.

Electroluminescence

In some films of GaP grown on GaAs substrates, light emission was noted. A broad-band emission was noted when the metal was made negative with respect to the film. A weak, orange emission was noted for the opposite polarity which disappeared permanently above a certain current level.

The electroluminescent mechanism for the broad band emission is probably due to some avalanche process. The interface between the GaP film and the GaAs substrate forms a heterojunction and therefore may be rectifying. Under reverse-bias conditions, the avalanche process could occur. As pointed out earlier, Gershenzon and Mikulyak observed this type of emission in diffused

diodes. Avalanche-type emission has also been noted in silicon devices.

The character of the orange emission is difficult to describe because of its delicate nature. The color would suggest recombination in the GaP film and, perhaps, at the metal-film junction.

Summary

The objective of this investigation was to study the flash-evaporation method of growing films of GaAs and GaP. Films were grown under various different substrate temperatures, source temperatures, source-to-substrate distances and rates of deposition. Optical, x-ray and electrical analysis was used to evaluate the properties of the resulting films.

As determined by this experiment, crystalline films can be grown by flash evaporation. To have polycrystalline films, the type of substrate is unimportant. Glass substrates, for instance, though amorphous, were sufficient to produce crystalline films. What was important was the substrate temperature. The division between amorphous films depended on the type of substrate but generally fell in the 250°C range.

The stoichiometry of the films was determined using x-ray fluorescence. To the degree of resolution

possible, the films appeared to be in the proper 1:1 ratio of gallium to arsenic.

The optical data showed that the band gap of the films grown on sapphire substrates generally fell in the expected range. There was a variation in the band gap energy measured which may be explained by either experimental error or actual band gap energy gap differences due to strains and doping.

The band gap is affected by the doping of the films. As doping is increased in n-type GaAs, for instance, the lower lying conduction levels are rapidly filled, so for an electron in the valence band to be excited into the conduction band, the photon energy required is not only the gap energy but an additional amount equal to that required to get above the lower, filled levels. The excitation energy, then, is increased by increased doping.

Strains tend to alter the band gap, as discussed previously in the optical section. The flattening of the edge was explained by the inhomogeneous distribution of strains. It must also be noted that the average band gap need not be equal to the bulk band gap, as it may be shifted in either direction by the strains.

Films grown from normally available material were very high in resistivity. Resistivity measurements

could not be made on those grown on semiconductor substrates, as the parallel conductive path through the substrate made meaningful measurements impossible. This is easily understood when one considers that it is practically impossible to place two leads on the film surface at a distance even approaching the thickness of the film. The path of least resistance would then be through the film, across the substrate and back up through the film which, if the probe placement is much greater than one micron, would be much less than the resistance across the film.

Films deposited on insulating substrates allowed resistance measurements to be made. Those obtained using normally available source materials showed less than one microampere at 200 volts.

In vacuum-deposited films of germanium and silicon, an annealing step is required for such films to have reasonable resistivities. As grown films show near intrinsic resistivity values. The annealing temperatures are quite high and a minimum is noted, below which annealing has very little effect. For silicon this minimum is in the order of 650°C, while for germanium it is about 250°C.

It follows that annealing of the films of GaAs and GaP grown in this experiment is in order to obtain

low-resistivity films. This was attempted. However, no appreciable changes in resistivity were noted at annealing temperatures of 400°C for over 72 hours. Higher temperatures tended to deteriorate the films, probably by the outgassing of the group-V component.

The difficulty for annealing GaP and GaAs arises from the vapor pressure of the more volatile group-V component. To minimize outgassing, additional powders of GaP or GaAs were included in the annealing ampoule. However, clearly visible surface damage was noted in films annealed at 900°C and on sapphire substrates the films were completely evaporated off the substrate. So whereas annealing is an important step in reducing the resistivities of vacuum grown films of germanium and silicon, it is a difficult step for GaAs and GaP films.

Also due to the volatility of the group-V component, the use of substrate temperatures of higher than 600°C was made impractical. For vapor transport growth of GaAs and GaP films, substrate temperatures in the range of 700°C to 900°C are used. This is possible since the vapor pressure of the surrounding gas is high enough. In vacuum deposition, obviously, the surrounding pressure is much lower and, hence, the higher and more desirable substrate temperature cannot be used.

Source material with large amounts of dopant were

prepared to obtain lower resistance films. Depending on the amount and type of dopant, resistivities as low as 0.6 ohm-cm were grown. Resistivity measurements were made using a four-point probe system.

The resistivity-versus-temperature data showed that the slope of the curves in the intrinsic region for GaAs films were reasonably close to the theoretical band gap for GaAs. The variation can again be explained in terms of dislocations and strains.

Diode fabrication was attempted using the flash-evaporated films. Films highly doped with tin and grown on sapphire substrates made ohmic contacts regardless of whether zinc or tin was used to make an alloyed contact. Point contacts, however, made rectifying junctions although the reverse characteristics were very poor.

Films were grown from evaporant material with high tin percentage on p-type substrates. The results showed that rectification did take place, but as in the point contact case, the reverse characteristics exhibited very high leakage currents.

Electroluminescence was observed on high-resistivity GaP films. The emission is probably due to some type of avalanche process since a broad output spectrum is seen. Whether the process is due to tunnelling across the high-resistivity region or whether it is due

to injection across the heterojunction was not resolved. However, since the luminescence occurred only on GaP films the second mechanism seems more likely.

The results of this investigation, then, show that for vacuum deposited films of GaAs and GaP, proper crystallinity and stoichiometry can be obtained. Optical and electrical methods show that the band gaps are near the theoretical value. However, due to the volatility of the group-V component, annealing and growth at higher substrate temperatures are difficult, if not impossible. Diodes grown by this method have too large a reverse leakage to be of practical use.

BIBLIOGRAPHY

1. Abrahams, M. S. and C. J. Burocchi. Etching of dislocations on the low-index faces of GaAs. Journal of Applied Physics 36:2855-2863. 1965.

2. Addamiano, A. Preparation of phosphides of Al, Ga and In. Journal of the American Chemical Society 82:1537-1540. 1960.

3. Allen, J. W. and P. E. Gibbons. Breakdown and light emission in GaP diodes. Journal of Electronics and Control 7:518-522. 1959.

4. Allen, J. W., M. E. Moncaster and J. Starkiewicz. Electroluminescent devices using carrier injection in gallium phosphide. Solid State Electronics 6:95-102. 1963.

5. Amsterdan, M. F. Surface effects in gallium arsenide. Semiconductor Products and Solid State Technology 9:15-19. 1966.

6. Anderson, R. L. Germanium-gallium arsenide hetero-junctions. IBM Journal of Research and Development 4:283-287. 1960.

7. Antell, G. R. and D. Effer. Preparation of crystals of InAs, InP, GaAs and GaP by a vapor phase reaction. Journal of the Electrochemical Society 106:509-511. 1959.

8. Braun, L. and D. E. Lood. Precision thin-film cermet resistors for integrated circuits. Proceedings of the Institute of Electrical and Electronic Engineers 54:1521-1527. 1966.

9. Braunstein, R. and L. Magid. Optical absorption in p-type GaAs. Physical Review 111:480-481. 1958.

10. Cunnel, F. A., J. T. Edmond and W. R. Harding. Technology of GaAs. Solid State Electronics 1:97-106. 1960.

11. Davey, J. E. and T. Pankey. Structural and optical characteristics of thin GaAs films. Journal of Applied Physics 35:2203-2209. 1964.

12. Eastman, P. D., R. R. Haering and P. A. Barnes. Injection electroluminescence in metal-semiconductor tunnel diodes. Solid State Electronics 7:879-885. 1964.

13. Effer, D. Epitaxial growth of doped and pure GaAs in open flow systems. Journal of the Electrochemical Society 112:1024-1025. 1965.

14. Effer, D. and G. R. Antell. Preparation of InAs, InP, GaAs and GaP by chemical methods. Journal of the Electrochemical Society 107:252-253. 1960.

15. Evans, R. C. An introduction to crystal chemistry. Cambridge, University Press, 1952. 388 p.

16. Gatos, Harry C. (ed.) Properties of elemental and compound semiconductors. New York, Interscience, 1960. 340 p.

17. Gershenzon, M. et al. Electroluminescent recombinations near the energy gap in GaP diodes. Solid State Electronics 7:113-124. 1964.

18. Gibbons, J. F. and P. C. Prehm. Epitaxial vapor growth of III-V compounds. Stanford, 1963. 45 numb. leaves. (Stanford University. Stanford Electronics Laboratories. Technical Documentary Report no. RTD-TDR-63-4238 on Air Force contract AF 33(616) -7726, Project no. 4169.)

19. Gilmer, J. J. (ed.) The art and science of growing crystals. New York, Wiley, 1963. 493 p.

20. Glass, A. M. Optical absorption edge broadening of evaporated germanium films. Canadian Journal of Physics 43:1068-1073. 1965.

21. Gorton, H. C., J. M. Swartz and C. S. Peet. Radiative recombination in GaP point-contact diodes. Nature (London) 188:303-304. 1960.

22. Grimmeiss, H. G. and H. Koelmans. pn Luminescence and photovoltic effects in GaP. Phillips Research Reports 15:290-304. 1960.

23. Grimmeiss, H. G. and H. Scholz. Efficiency of recombination radiation in GaP. Physical Review Letters 8:233. 1964.

24. Hannay, N. B. Semiconductors. New York, Reinhold, 1959. 767 p.

25. Hewlett-Packard Associates. Interim engineering report for semiconductor materials, no. 6, July 1965 to October 1965. Palo Alto, 1965. 42 numb. leaves. (Contract no. NObsr-89489 of Department of Navy, Bureau of Ships.)

26. Hoffman, James I. Preparation of pure gallium. Journal of Research of the National Bureau of Standards 13:665-672. 1934.

27. Holland, L. Vacuum deposition of thin films. London, Chapman, 1961. 542 p.

28. Holt, D. A., G. F. Alfrey and C. S. Wiggins. Grain boundaries and electroluminescence in GaP. Nature (London) 181:109. 1958.

29. Humphris, R. R. and A. Catlin. Role of surface states in contributing to p-type carrier concentration of vacuum deposited thin germanium films. Solid State Electronics 8:957-960. 1965.

30. Jaccodine, R. J. Interaction of diffusion and stacking faults in silicon epitaxial material. Journal of Applied Physics 36:2811-2814. 1965.

31. Kittel, C. Introduction to solid state physics. New York, Wiley, 1963. 617 p.

32. Kolm, C., S. A. Kulin and B. L. Averbach. Studies on group III-V intermetallic compounds. Physical Review 108:965-971. 1957.

33. Kontsevoi, Yu. A. Methods of measuring electrical and physical parameters of epitaxial semiconductor films. Instruments and Experimental Techniques 1:1-10. 1965.

34. Kumagai, H. Y., J. M. Thompson and G. Krauss. Properties and structure of thin silicon film sputtered on fused quartz substrates. Transactions of the Metallurgical Society, of American Institute of Mining, Metallurgical and Petroleum Engineers 236:295-299. 1966.

35. Leite, R. C. C. et al. Injection mechanisms in GaAs diffused electroluminescent junctions. Physical Review 137:1583-1590. 1965.

36. Lever, R. F. and E. J. Huminski. Epitaxy of germanium films on GaAs by vacuum evaporation. Journal of Applied Physics 37:3638-3639. 1966.

37. Loebner, E. E. and E. W. Poor. Bimolecular electroluminescent transitions in GaP. Physical Review Letters 3:23-25. 1959.

38. Madelung, Otfried. Physics of III-V Compounds. New York, Wiley, 1964. 409 p.

39. Molnar, B., J. J. Flood and M. H. Francombe. Fibered and epitaxial growth in sputtered films of GaAs. Journal of Applied Physics 35:3554-3559. 1964.

40. Moss, T. S. Optical properties of semiconductors. London, Butterworth, 1959. 279 p.

41. Müller, E. K. and J. L. Richards. Miscibility of III-V semiconductors studied by flash evaporation. Journal of Applied Physics 35:1233-1240. 1964.

42. Powell, R. W. Some anisotropic properties of gallium. Nature (London) 164:153-154. 1949.

43. Richards, J. L., P. B. Hart and L. M. Gallone. Epitaxy of compound semiconductors by flash evaporation. Journal of Applied Physics 34:3418-3420. 1963.

44. Rosenbert, R. et al. Strain patterns in $GaAs_{(1-x)}P_x$ alloy overgrowths. Journal of the Electrochemical Society 112:459-461. 1965.

45. Ryvkin, Solomon M. Photoelectric effects in semiconductors. New York, Consultants Bureau, 1964. 402 p.

46. Shockley, W. et al. (eds.) Imperfections in nearly perfect crystals. New York, Wiley, 1952. 490 p.

47. Spitzer, W. G. and J. M. Whelan. Infrared absorption and electron effective mass in n-type GaAs. Physical Review 114:59-63. 1959.

48. Starkiewicz, J. and J. W. Allen. Injection electroluminescence at pn junctions in zinc-doped gallium phosphide. Journal of Physics and Chemistry 23:881-884. 1962.

49. Stern, F. and R. M. Tallay. Impurity band in semiconductors with small effective mass. Physical Review 100:1638-1643. 1955.

50. van Wyk, J. D. Visible electroluminescence from base-emitter pn junctions of avalanching silicon transistors. Solid State Electronics 8:803-805. 1965.

51. Welker, H. Optical and electrical properties of GaAs, InP and GaP. Journal of Electronics 1:181-185. 1955.

52. Willardson, Robert K. and H. Goering (eds.) Compound semiconductors Vol. 1. New York, Reinhold, 1962. 553 p.

53. Wolff, G. A., R. A. Herbert and J. D. Broder. Electroluminescence of GaP. Physical Review 100:1144-1145. 1955.